

Electronic Supporting information

Synthesis and reactivity of 9,10-bis(4-trimethylsilyl-ethynylbuta-1,3-diynyl)anthracene derived chromophores

Benjamin J. Frogley and Anthony F. Hill

General Experimental Conditions and Instrumentation - Unless otherwise stated, experimental work was carried out at room temperature under a dry and oxygen-free nitrogen atmosphere using standard Schlenk techniques with dried and degassed solvents.

NMR spectra were obtained on a Bruker Avance 400 (^1H at 400.1 MHz, ^{13}C at 100.6 MHz, ^{31}P at 162.0 or a Bruker Avance 700 (^1H at 700.0 MHz, ^{13}C at 176.1 MHz) spectrometers at the temperatures indicated. Chemical shifts (δ) are reported in ppm with coupling constants given in Hz and are referenced to the protio-impurity (^1H), the deuterated solvent itself (^{13}C), or externally referenced (CFCl_3 for $^{19}\text{F}\{^1\text{H}\}$, 85% H_3PO_4 in H_2O for $^{31}\text{P}\{^1\text{H}\}$). The multiplicities of NMR resonances are denoted by the abbreviations s (singlet), d (doublet), t (triplet), m (multiplet), br (broad) and combinations thereof for more highly coupled systems. In some cases, distinct peaks were observed in the ^1H and $^{13}\text{C}\{^1\text{H}\}$ NMR spectra, but to the level of accuracy that is reportable (i.e. 2 decimal places for ^1H NMR, 1 decimal place for ^{13}C NMR) they are reported as having the same chemical shift. The abbreviation ‘pz’ is used to refer to the pyrazolyl rings on the hydrotris(3,5-dimethylpyrazol-1-yl)borate (Tp^*) ligand. Spectra provided generally correspond to samples obtained directly from chromatography and may contain residual solvent as recrystallised samples often display reduced solubility.

Infrared spectra were obtained using a Shimadzu FTIR-8400 spectrometer. The strengths of IR absorptions are denoted by the abbreviations vs (very strong), s (strong), m (medium), w (weak), sh (shoulder) and br (broad). UV/Vis data were collected from solutions in 1 cm quartz cells using a PerkinElmer Lambda 465 spectrophotometer. Fluorescence data were collected on a Varian Cary Eclipse fluorescence spectrophotometer. Elemental microanalytical data were provided the London Metropolitan University or Macquarie University microanalytical services. High-resolution electrospray ionisation mass spectrometry (ESI-MS) was performed by the ANU Research School of Chemistry mass spectrometry service with acetonitrile or methanol as the matrix.

Data for X-ray crystallography were collected with an Agilent SuperNova CCD diffractometer using Cu-K α

radiation ($\lambda = 1.54184 \text{ \AA}$) and the CrysAlis PRO software.¹ The structures were solved by intrinsic phasing methods and refined by full-matrix least-squares on F^2 using the SHELXT and SHELXL programs.² Hydrogen atoms were located geometrically and refined using a riding model. Diagrams were produced using the CCDC visualisation program Mercury.³ Structural data for 9,10-bis(phenylbuta-1,3-diynyl)anthracene (**5**) were collected at the Australian Synchrotron using the MX1 beamline using silicon double crystal monochromated synchrotron radiation at 100 K. Raw frame data were collected using BluIce⁴ and data reduction, interframe scaling, unit cell refinement and absorption corrections were processed using XDS.⁵ Crystallographic data for complexes described herein may be obtained from the Cambridge Crystallographic Data Centre CCDC 2231630-2231635.

Computational studies were performed by using the SPARTAN20® suite of programs.⁶ Geometry optimisation (gas phase) was performed at the DFT level of theory using the ω B97X-D exchange functionals of Head-Gordon.⁷ The Los Alamos effective core potential type basis set (LANL2D \square) of Hay and Wadt⁸ was used for Au while Pople 6-31G* basis sets⁹ were used for all other atoms. Frequency calculations were performed for all compounds to confirm that each optimized structure was a local minimum and also to identify vibrational modes of interest. Cartesian atomic coordinates are provided below.

References

- 1 Agilent, *CrysAlis PRO*, Agilent Technologies Ltd, Yarnton, Oxfordshire, England, 2014.
- 2 (a) G. Sheldrick, *Acta Crystallogr. Sect. A: Found. Crystallogr.*, 2008, **64**, 112-122; (b) G. M. Sheldrick, *Acta Crystallogr. Sect. C: Cryst. Struct. Commun.*, 2015, **71**, 3-8.
- 3 (a) C. F. Macrae, P. R. Edgington, P. McCabe, E. Pidcock, G. P. Shields, R. Taylor, M. Towler and J. van de Streek, *J. Appl. Crystallogr.*, 2006, **39**, 453-457; (b) C. F. Macrae, I. J. Bruno, J. A. Chisholm, P. R. Edgington, P. McCabe, E. Pidcock, L. Rodriguez-Monge, R. Taylor, J. van de Streek and P. A. Wood, *J. Appl. Crystallogr.*, 2008, **41**, 466-470.
- 4 T. M. McPhillips, S. E. McPhillips, H.-J. Chiu, A. E. Cohen, A. M. Deacon, P. J. Ellis, E. Garman, A. Gonzalez, N. K. Sauter, R. P. Phizackerley, S. M. Soltis and P. Kuhn, *J. Synchrotron Rad.*, 2002, **9**, 401-406.
- 5 W. Kabsch, *J. Appl. Crystallogr.*, 1993, **26**, 795-800.
- 6 Spartan 20® (2020) Wavefunction, Inc., 18401 Von Karman Ave., Suite 370 Irvine, CA 92612 U.S.A.
- 7 (a) J. D. Chai and M. Head-Gordon, *J. Chem. Phys.*, 2008, **128**, 084106. (b) J. D. Chai and M. Head-Gordon, *Phys. Chem. Chem. Phys.*, 2008, 10, 6615-6620.
- 8 (a) P. J. Hay and W. R. Wadt, *J. Chem. Phys.*, 1985, **82**, 270-283. (b) P. J. Hay and W. R. Wadt, *J. Chem. Phys.*, 1985, **82**, 299-310. (c) W. R. Wadt and P. J. Hay, *J. Chem. Phys.*, 1985, **82**, 284-298.
- 9 W. J. Hehre, R. Ditchfield and J. A. Pople, *J. Chem. Phys.*, 1972, **56**, 2257-2261.

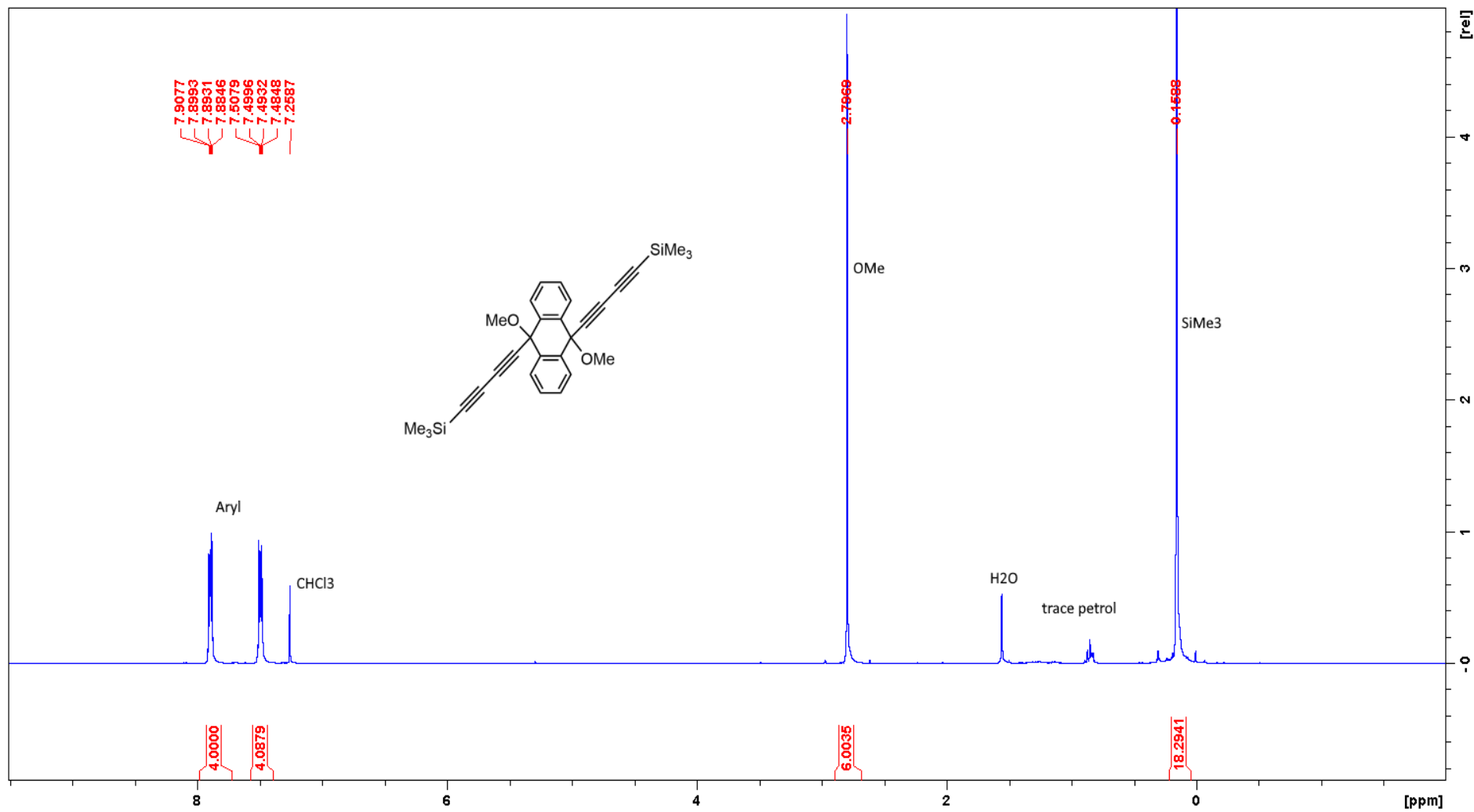


Figure S1. ^1H NMR (400 MHz, CDCl₃, 25°C, δ) of *trans*-9,10-dimethoxy-9,10-bis(trimethylsilylbut-1,3-diyne-1-yl)dihydroanthracene (**2**).

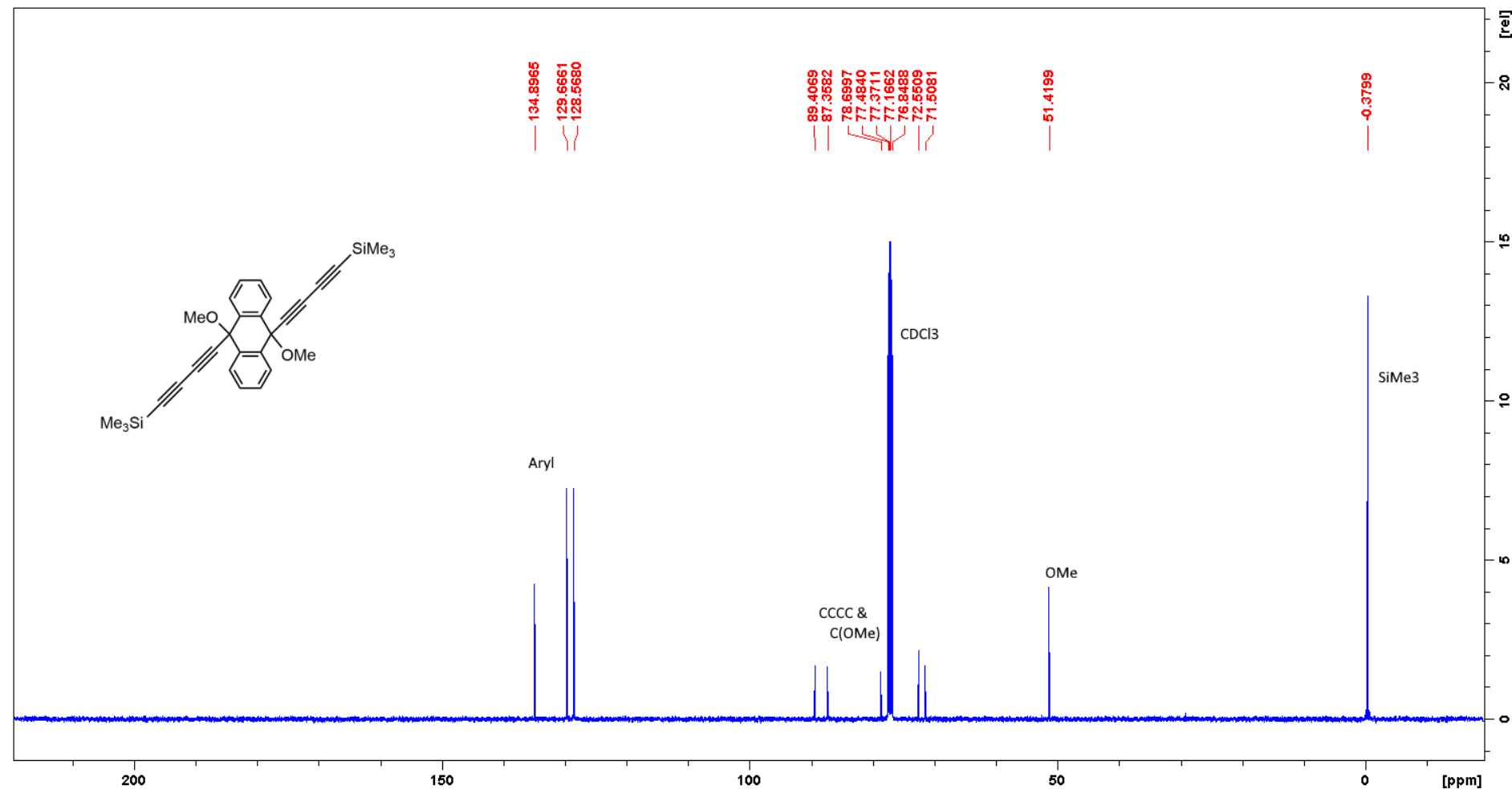


Figure S2. $^{13}\text{C}\{^1\text{H}\}$ NMR (75 MHz, CDCl₃, 25°C, δ) of *trans*-9,10-dimethoxy-9,10-bis(trimethylsilylbut-1,3-diyn-1-yl)dihydroanthracene (**2**).

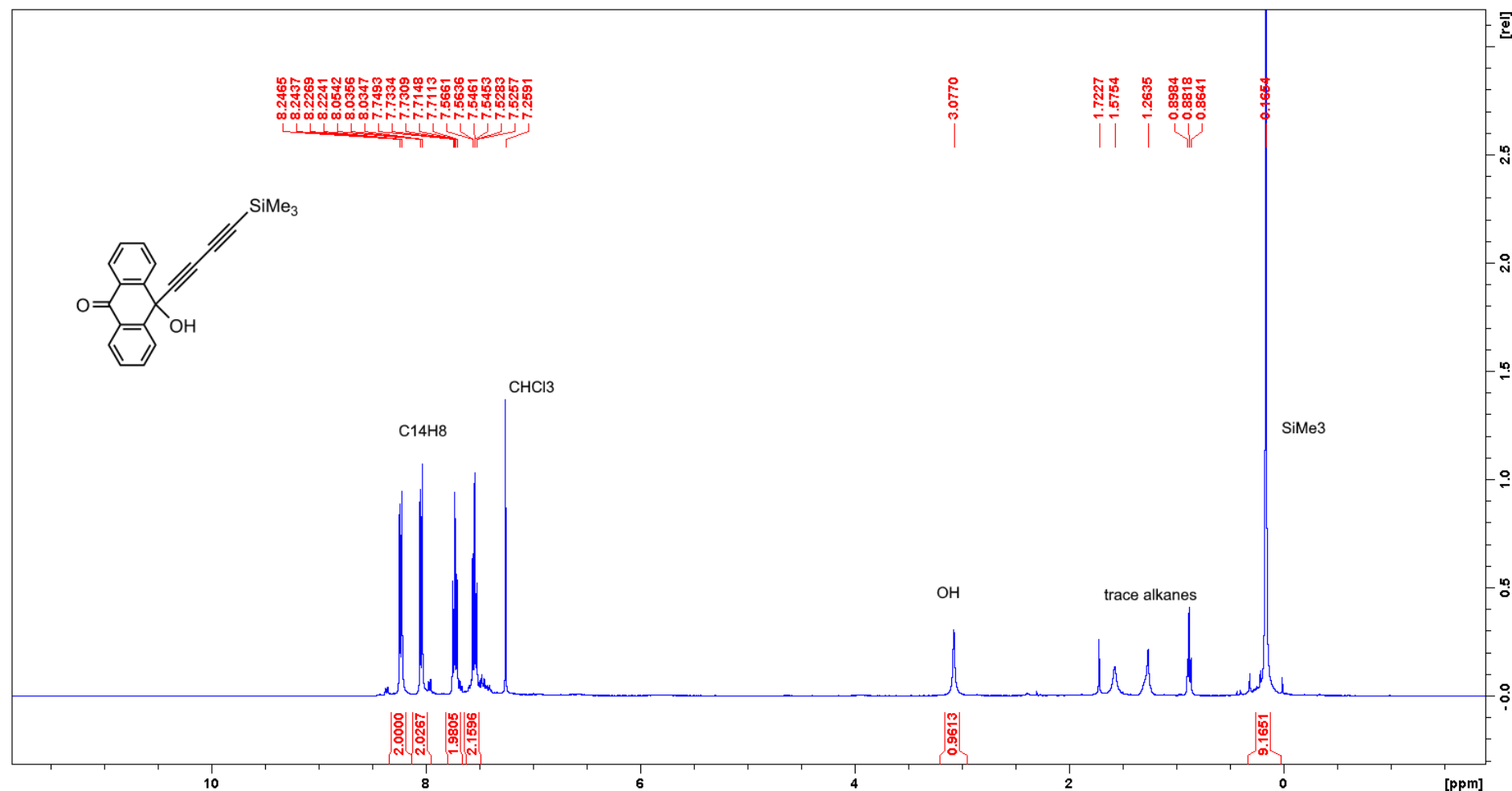


Figure S3. ^1H NMR (400 MHz, CDCl₃, 25°C, δ) of 10-hydroxy-10-(trimethylsilylbuta-1,3-diyen-1-yl)anthracen-9(10H)-one (3).

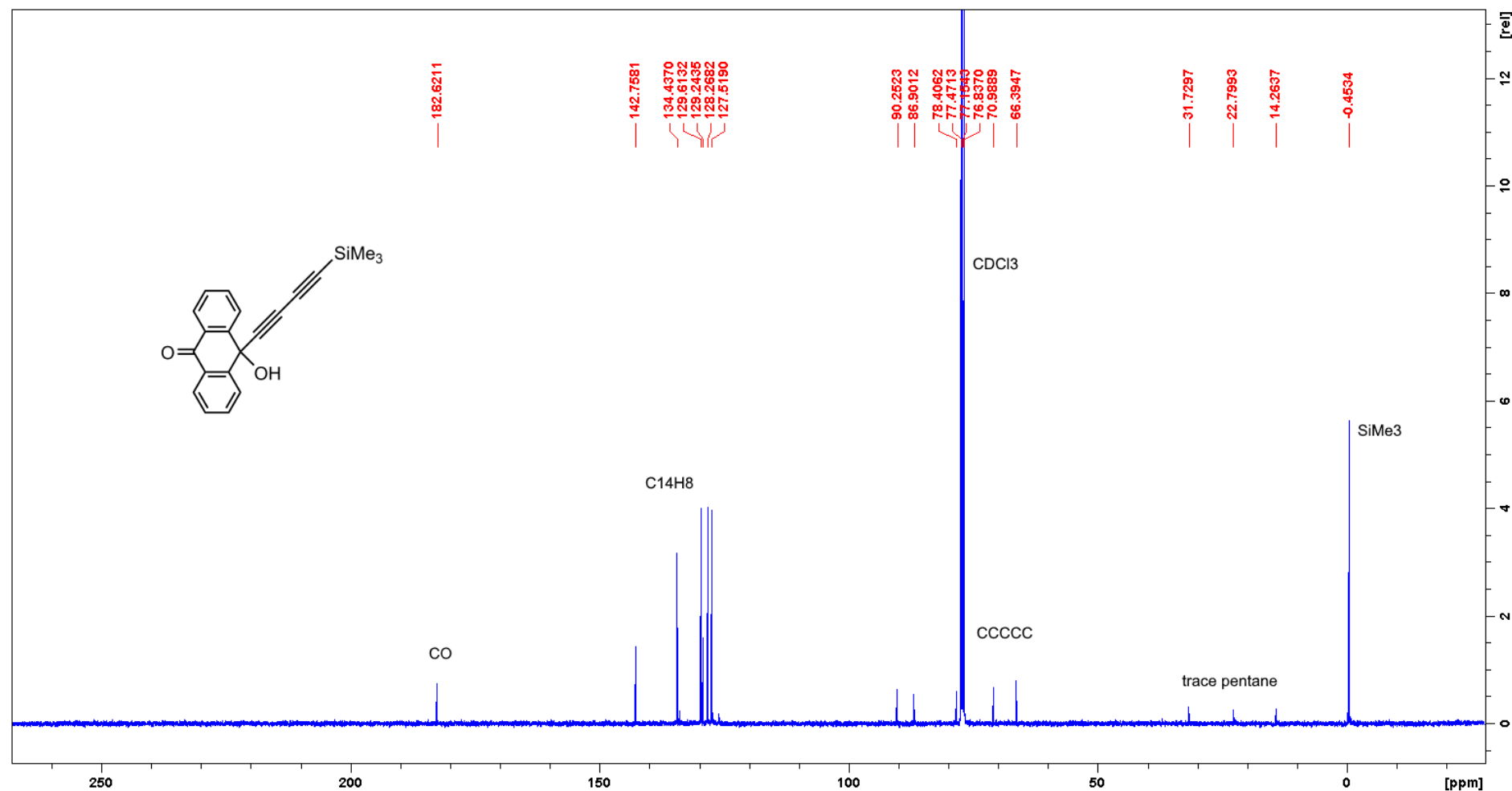


Figure S4. $^{13}\text{C}[^1\text{H}]$ NMR (101 MHz, CDCl_3 , 25°C, δ) of 10-hydroxy-10-(trimethylsilylbuta-1,3-dienyl)anthracen-9(10H)-one (3).

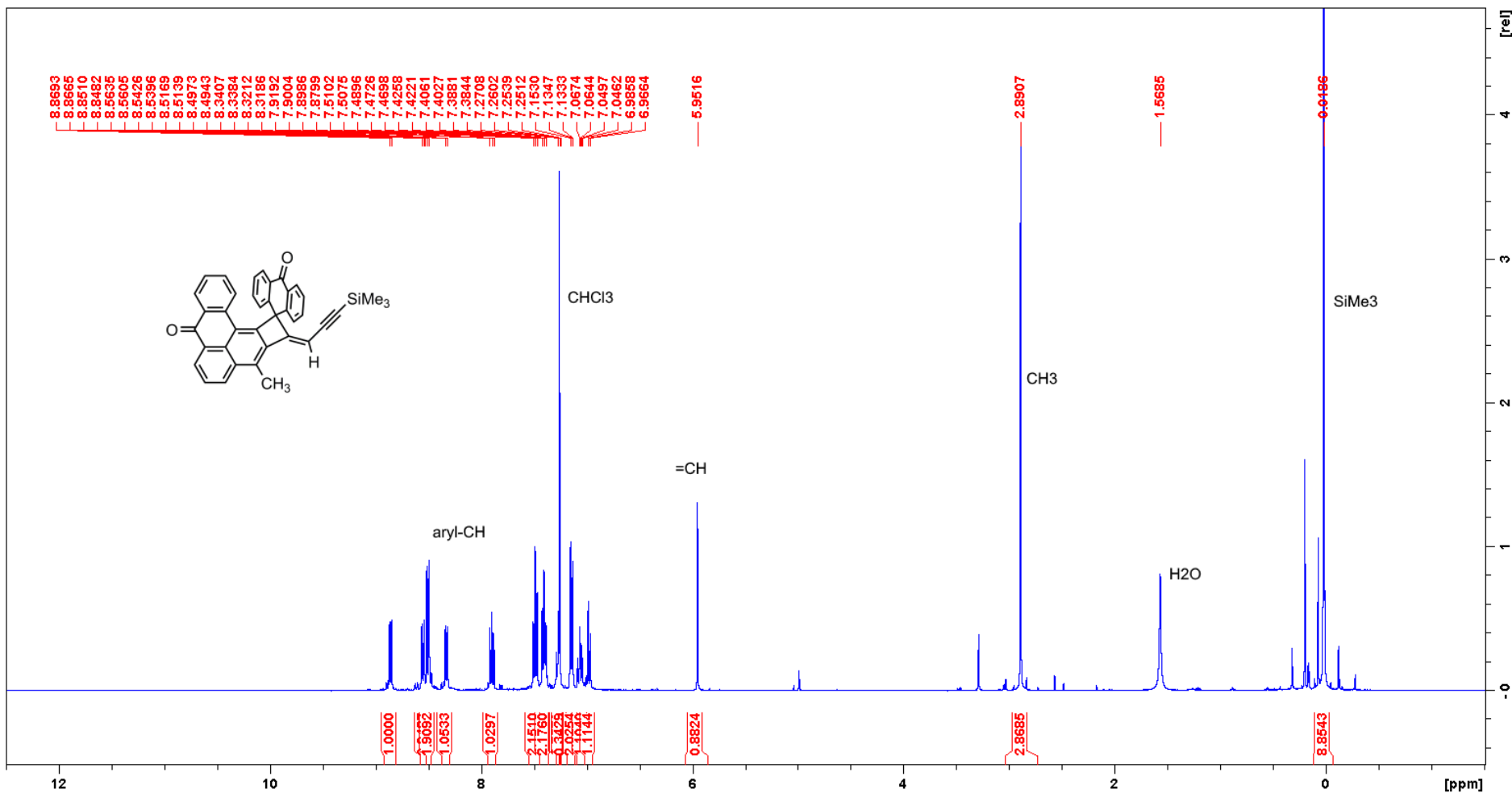
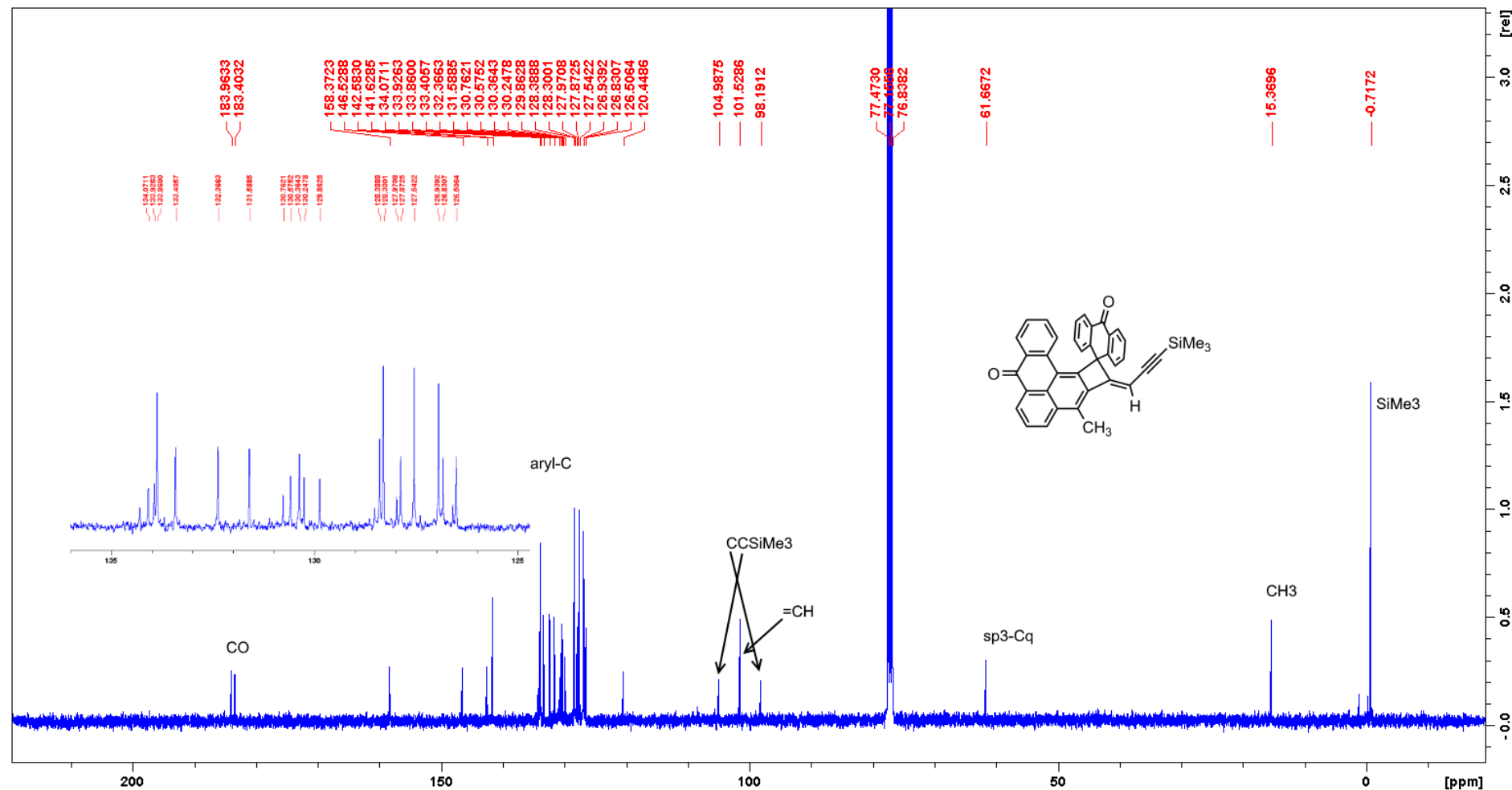


Figure S5. ^1H NMR (400 MHz, CDCl_3 , 25°C, δ) of the dimerization product (**4**).



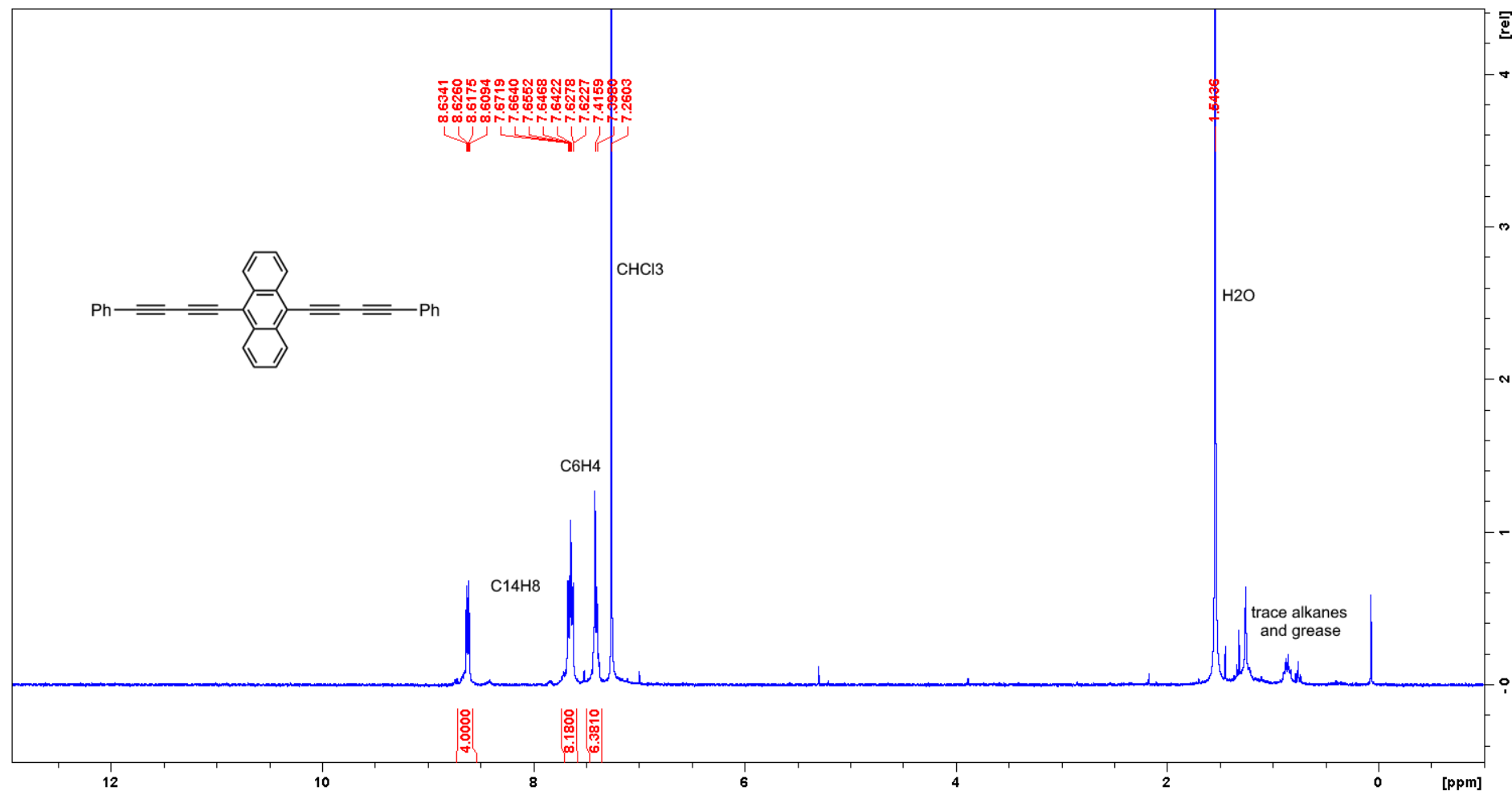


Figure S7. ^1H NMR (400 MHz, CDCl₃, 25°C, δ) of 9,10-bis(phenylbut-1,3-diyn-1-yl)anthracene (5).

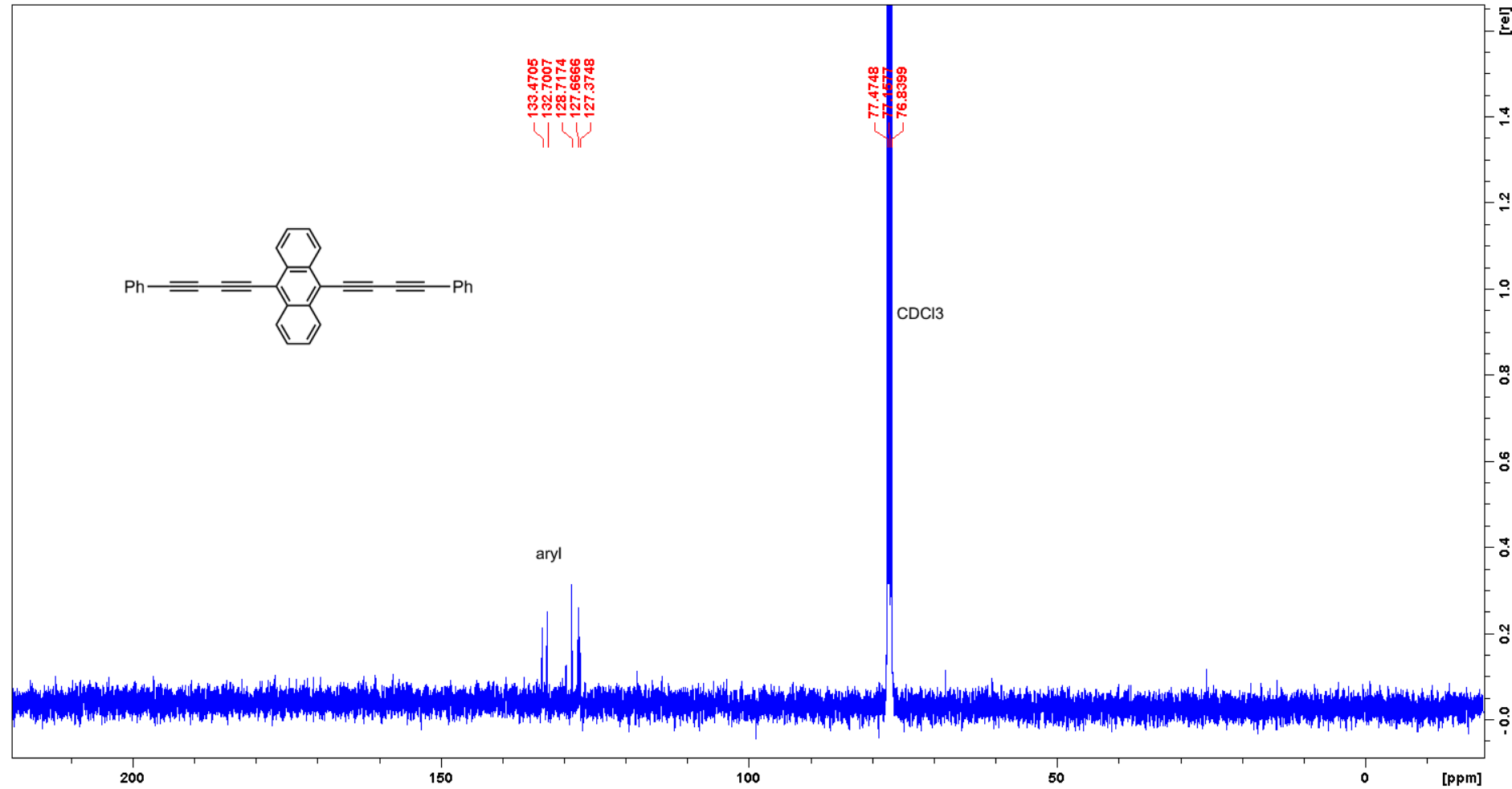


Figure S8. $^{13}\text{C}\{^1\text{H}\}$ NMR (101 MHz, CDCl₃, 25 °C, δ) of 9,10-bis(phenylbut-1,3-diyn-1-yl)anthracene (5).

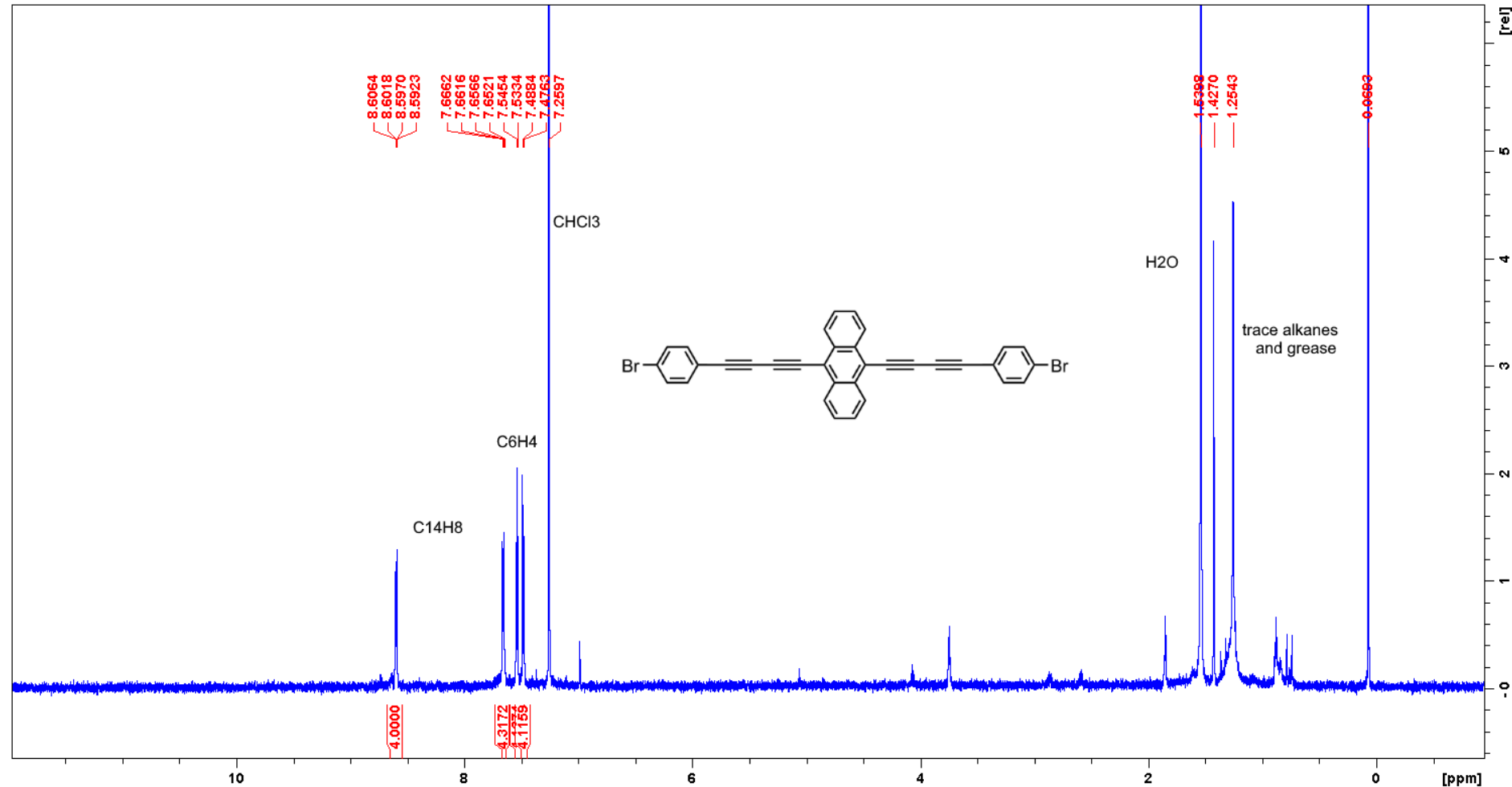


Figure S9. ^1H NMR (700 MHz, CDCl₃, 25°C, δ) of 9,10-bis((4-bromophenyl)but-1,3-dien-1-yl)anthracene (6).

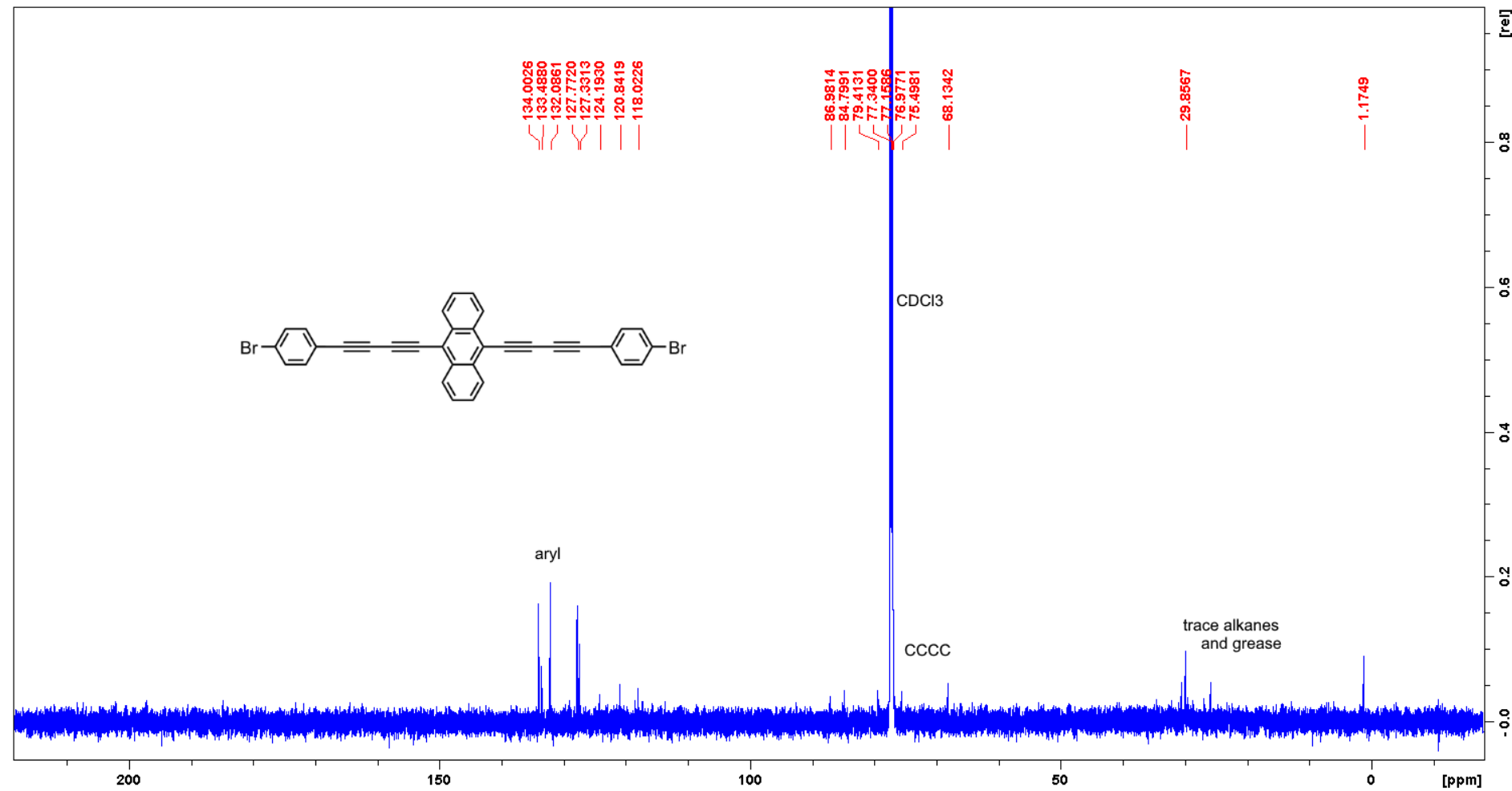


Figure S10. $^{13}\text{C}\{^1\text{H}\}$ NMR (176 MHz, CDCl₃, 25°C, δ) of 9,10-bis((4-bromophenyl)but-1,3-diyin-1-yl)anthracene (6).

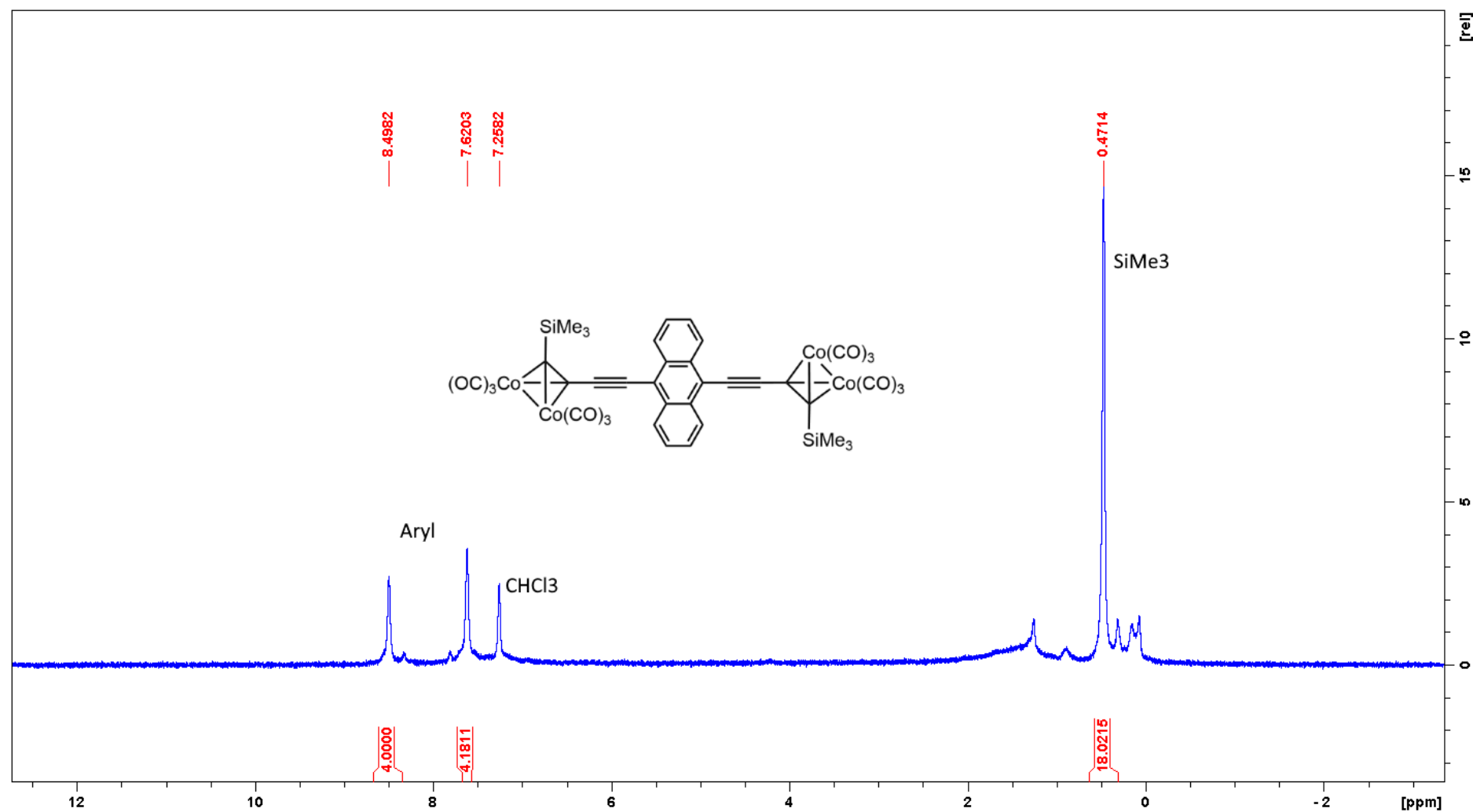


Figure S11. ^1H NMR (700 MHz, CDCl_3 , 25°C, δ) of the tetracobalt complex (7).

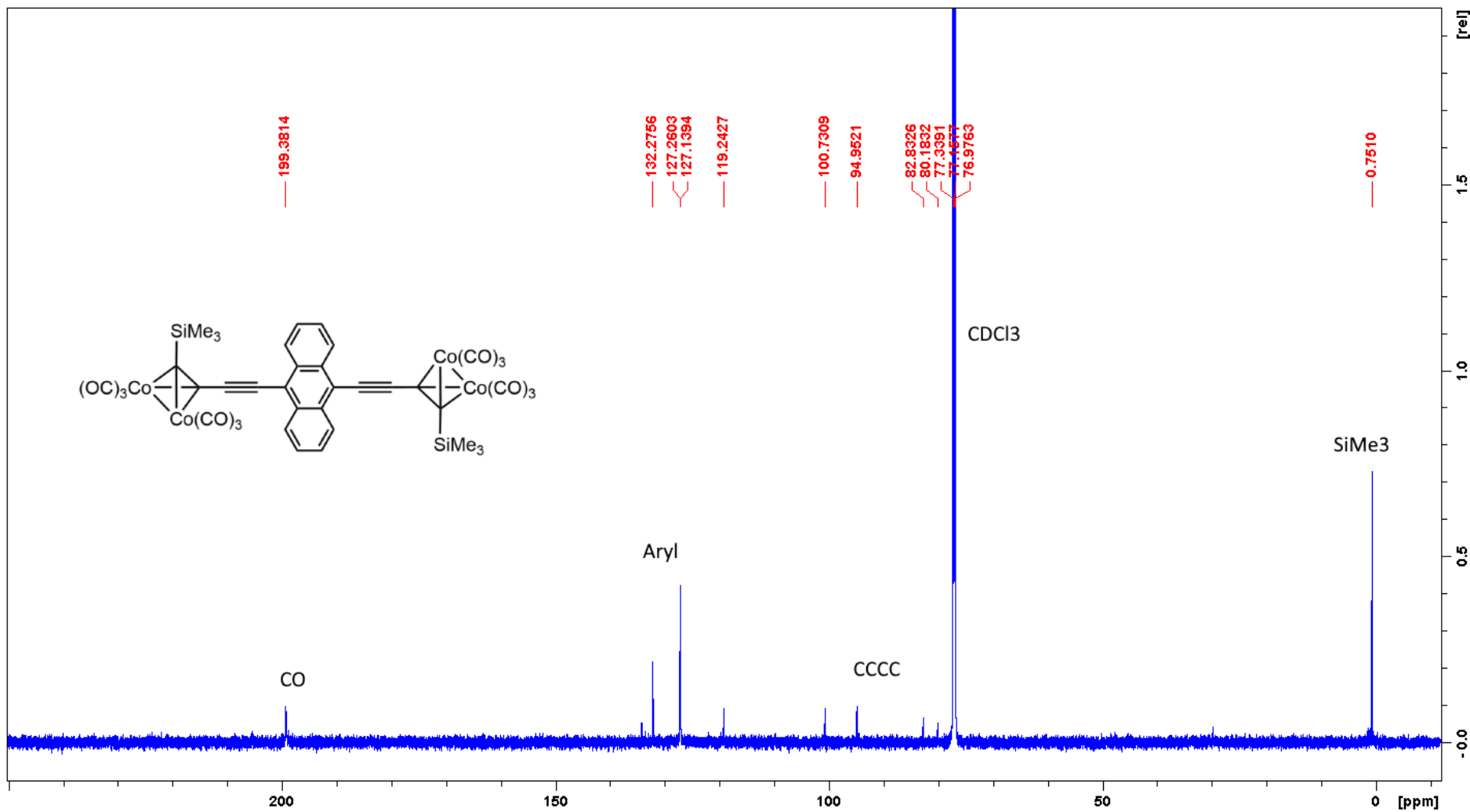


Figure S12. $^{13}\text{C}\{^1\text{H}\}$ NMR (176 MHz, CDCl_3 , 25°C, δ) of tetracobalt complex (7).

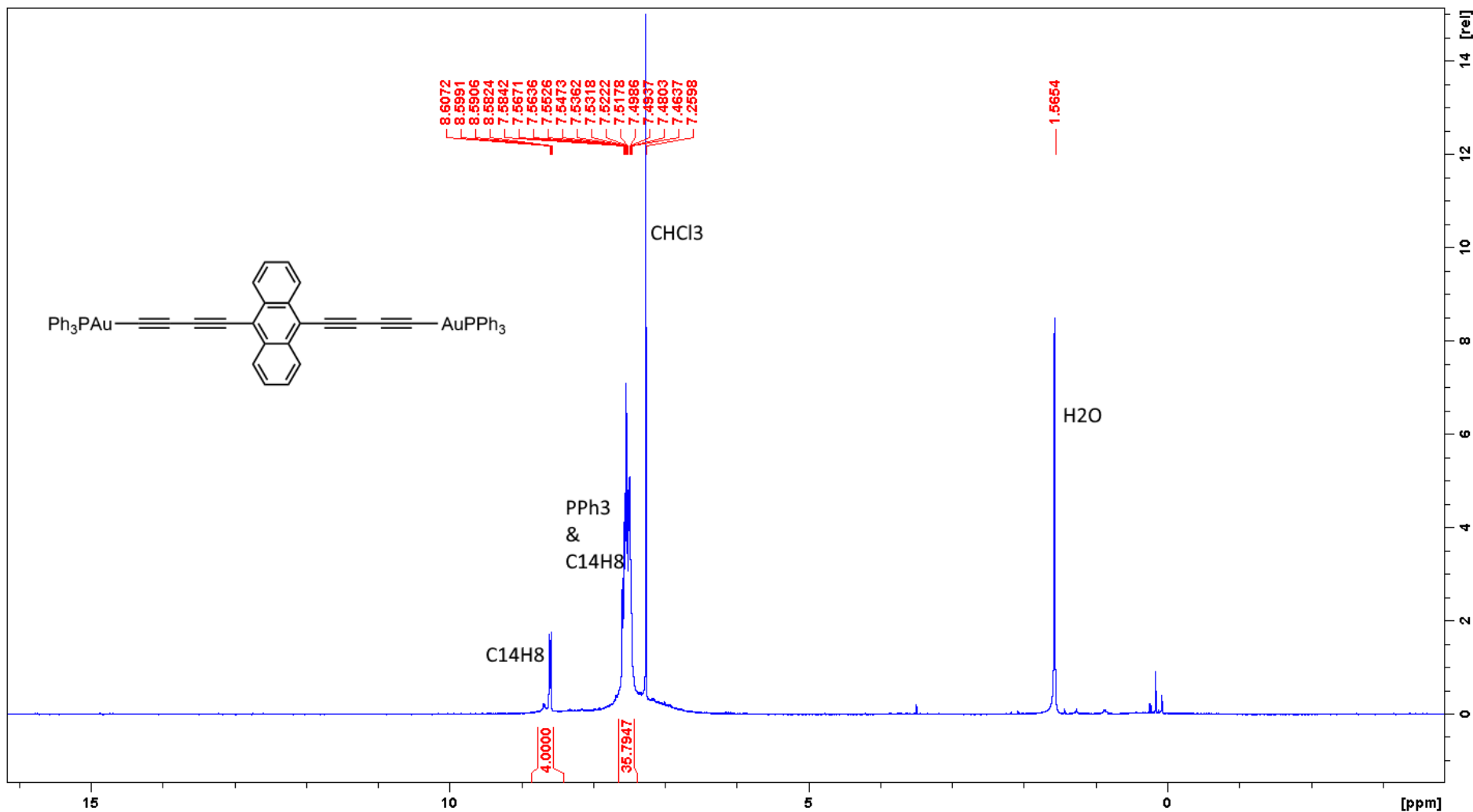


Figure S13. ¹H NMR (700 MHz, CDCl₃, 25 °C, δ) of 9,10-bis(triphenylphosphinegold-but-1,3-diyen-1-yl)anthracene (**8**).

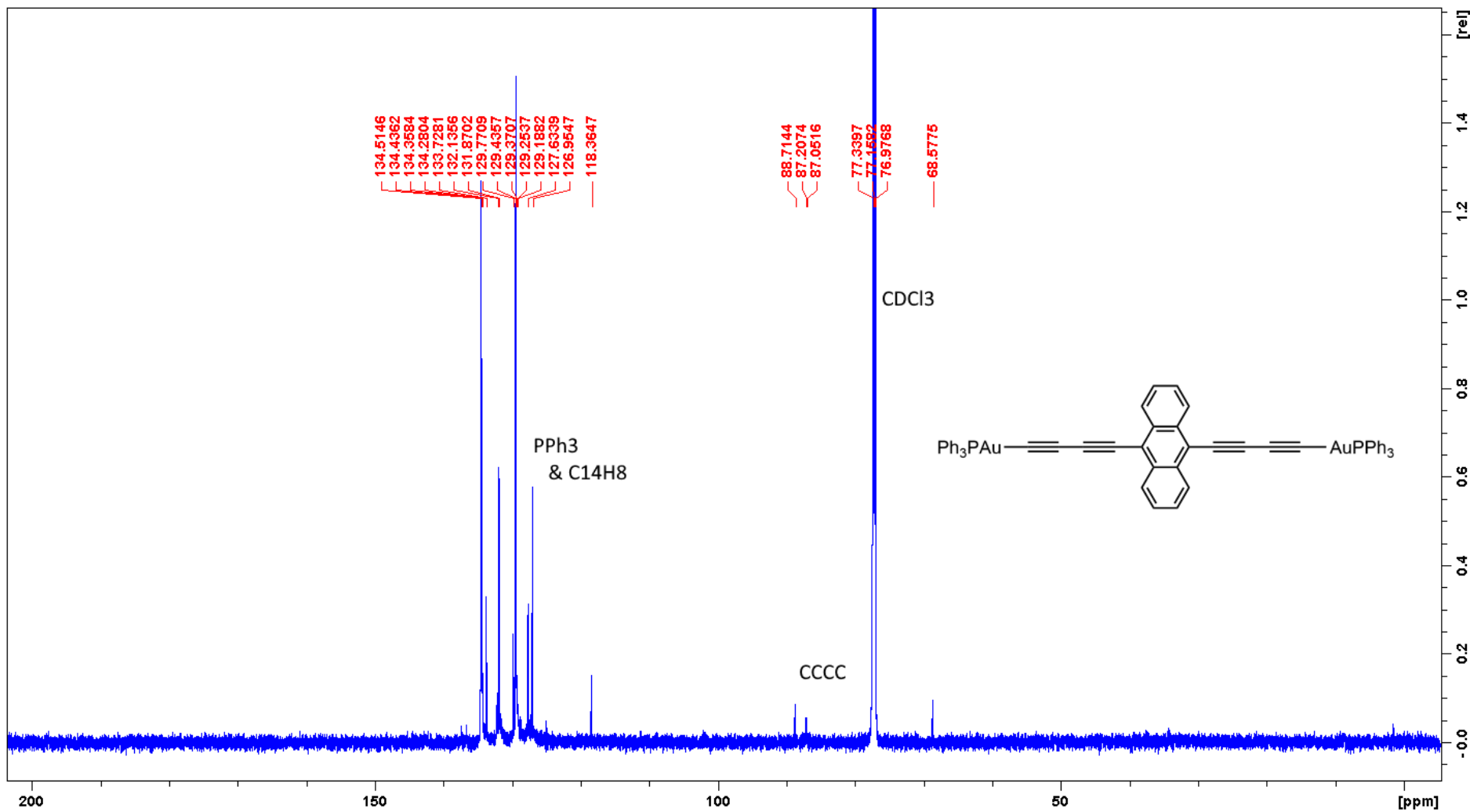


Figure S14. $^{13}\text{C}\{^1\text{H}\}$ NMR (176 MHz, CDCl_3 , 25°C, δ) of 9,10-bis(triphenylphosphinegold-buta-1,3-diyn-1-yl)anthracene (8).

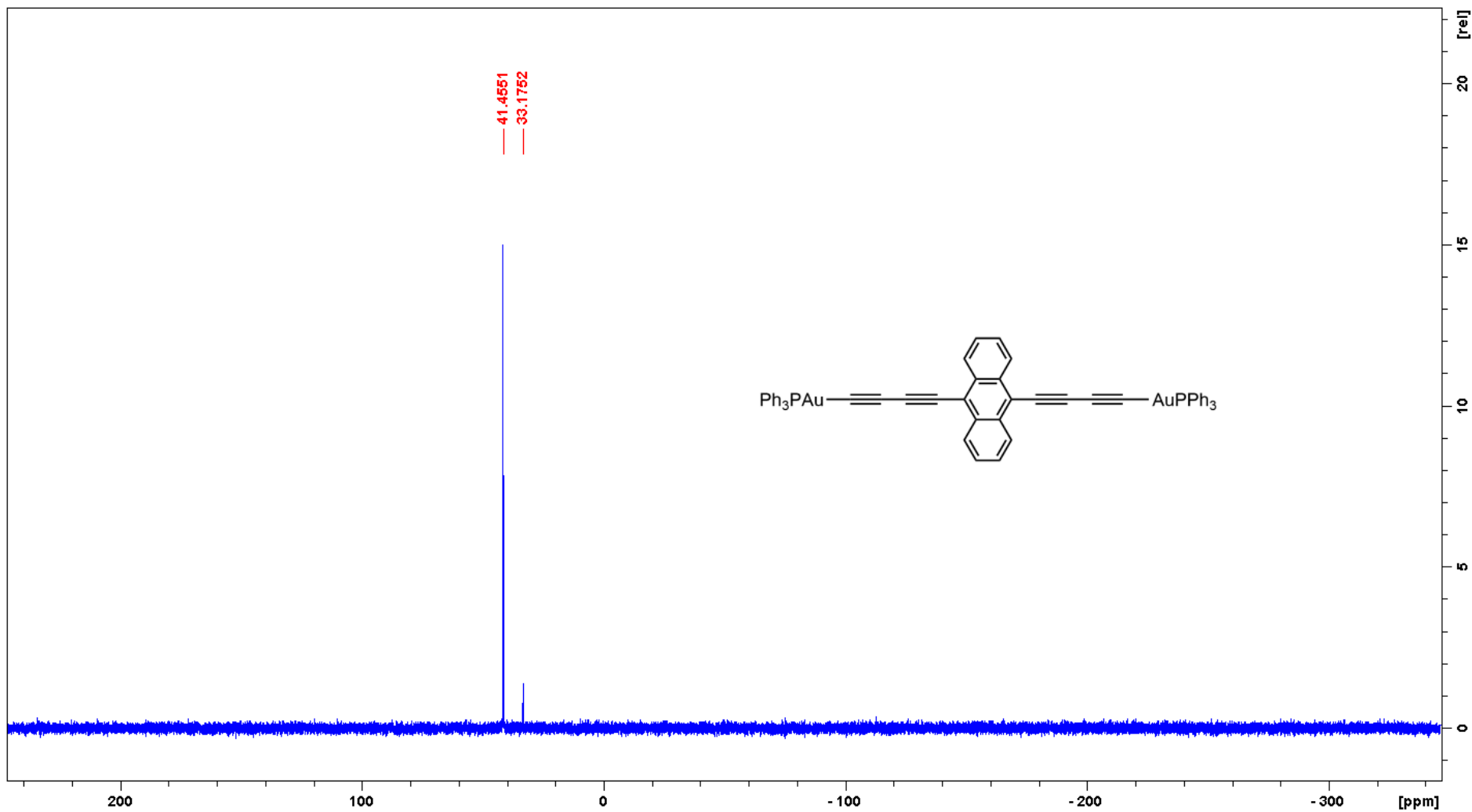


Figure S15. $^{31}\text{P}\{^1\text{H}\}$ NMR (162 MHz, CDCl_3 , 25°C, δ) of 9,10-bis(triphenylphosphinegold-but-1,3-diyen-1-yl)anthracene (8).

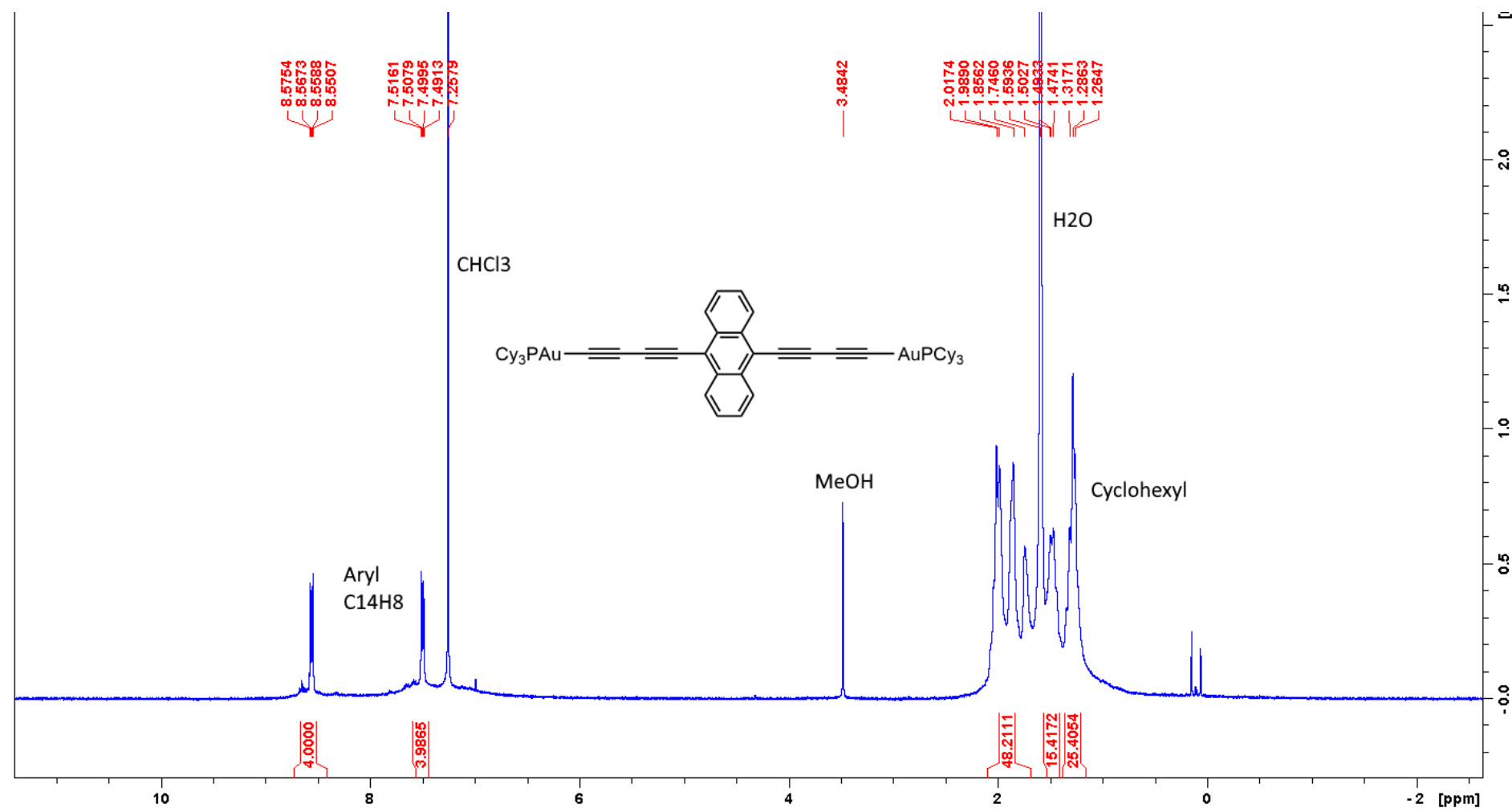


Figure S16. ^1H NMR (700 MHz, CDCl_3 , 25°C, δ) of 9,10-bis(tricyclohexylphosphinegold-but-1,3-diyn-1-yl)anthracene (9).

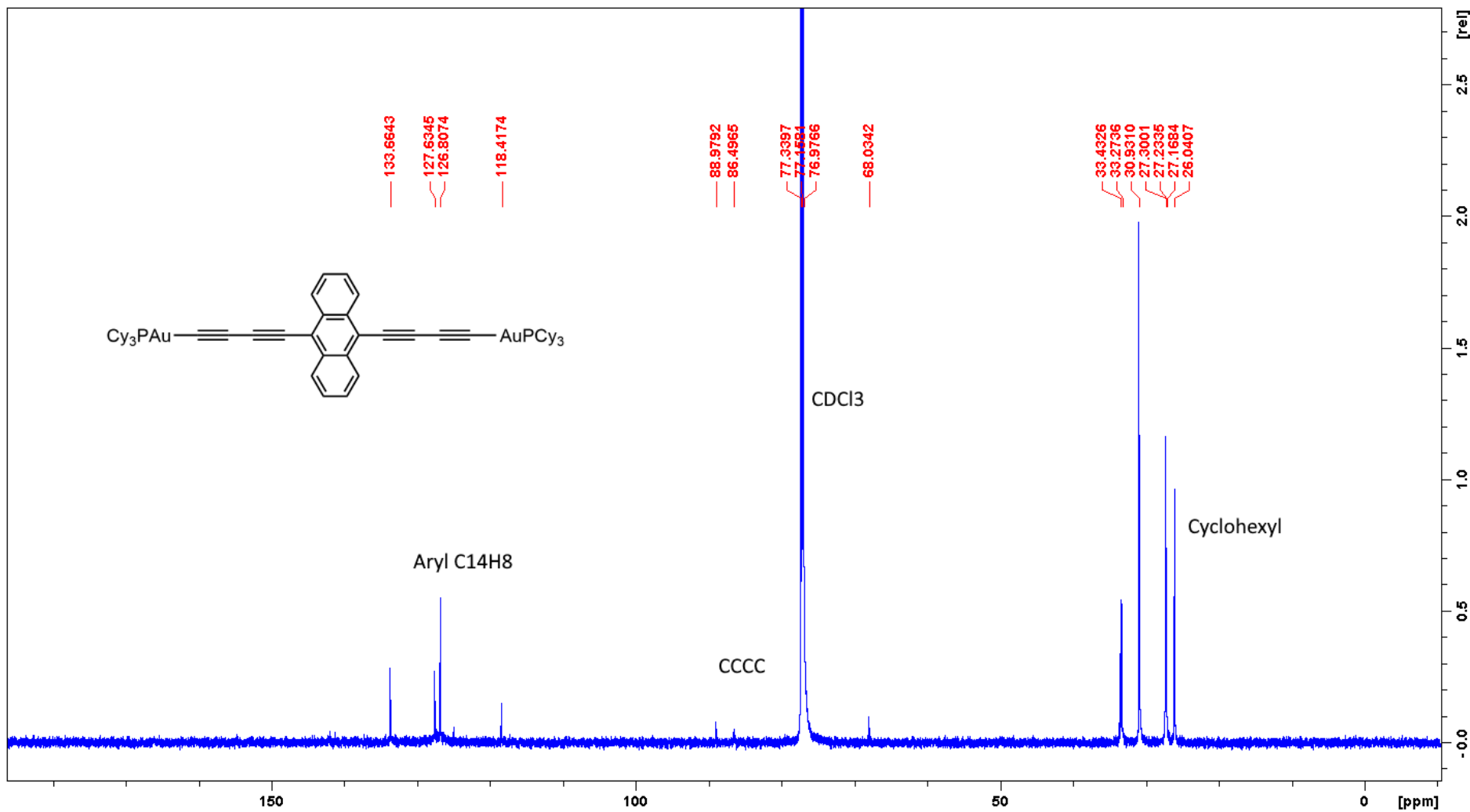


Figure S17. $^{13}\text{C}\{^1\text{H}\}$ NMR (176 MHz, CDCl₃, 25 °C, δ) of 9,10-bis(tricyclohexylphosphinegold-but-1,3-diyn-1-yl)anthracene (**9**).

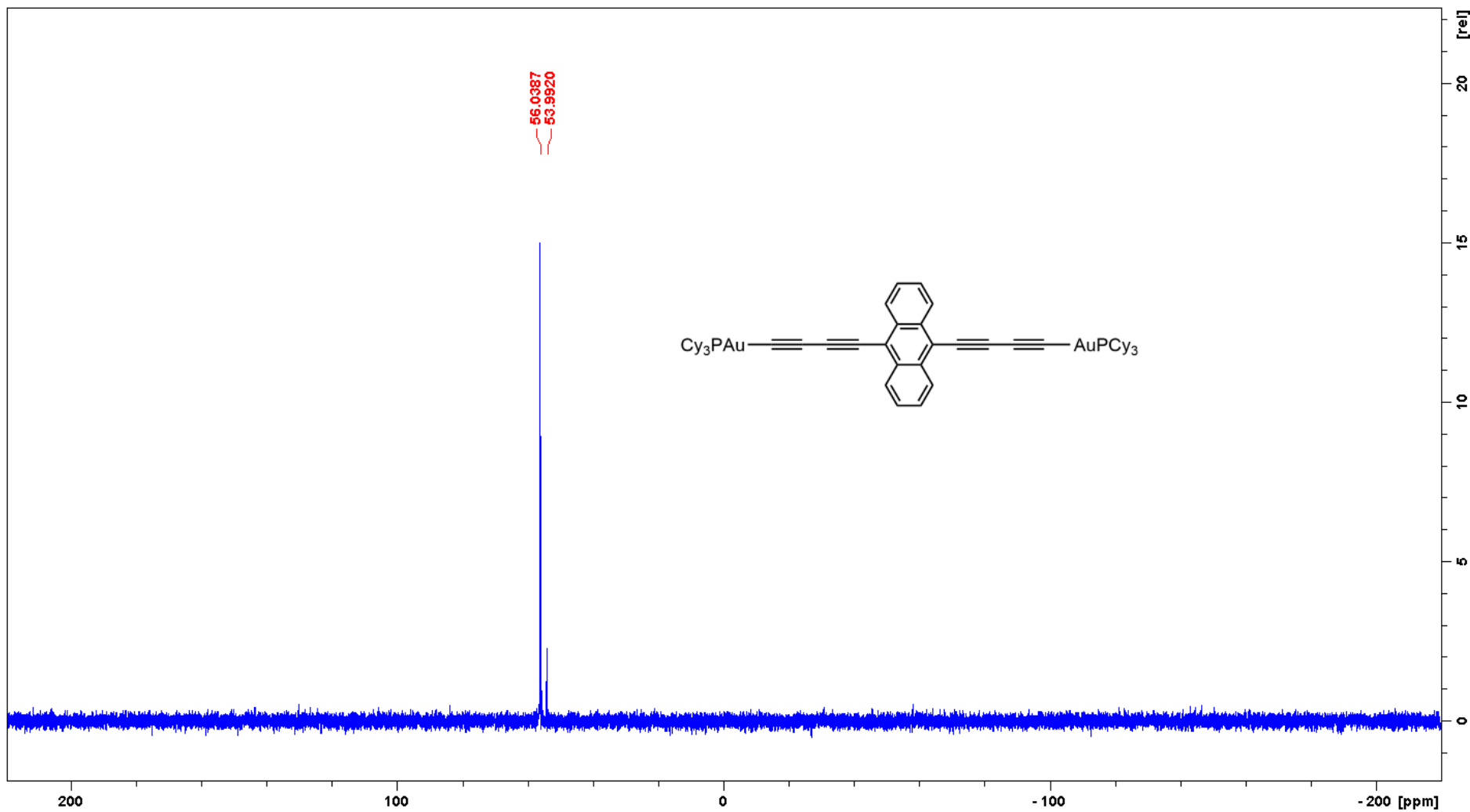


Figure S18. $^{31}\text{P}\{\text{H}\}$ NMR (162 MHz, CDCl_3 , 25°C, δ) of 9,10-bis(tricyclohexylphosphinegold-but-1,3-diyn-1-yl)anthracene (9).

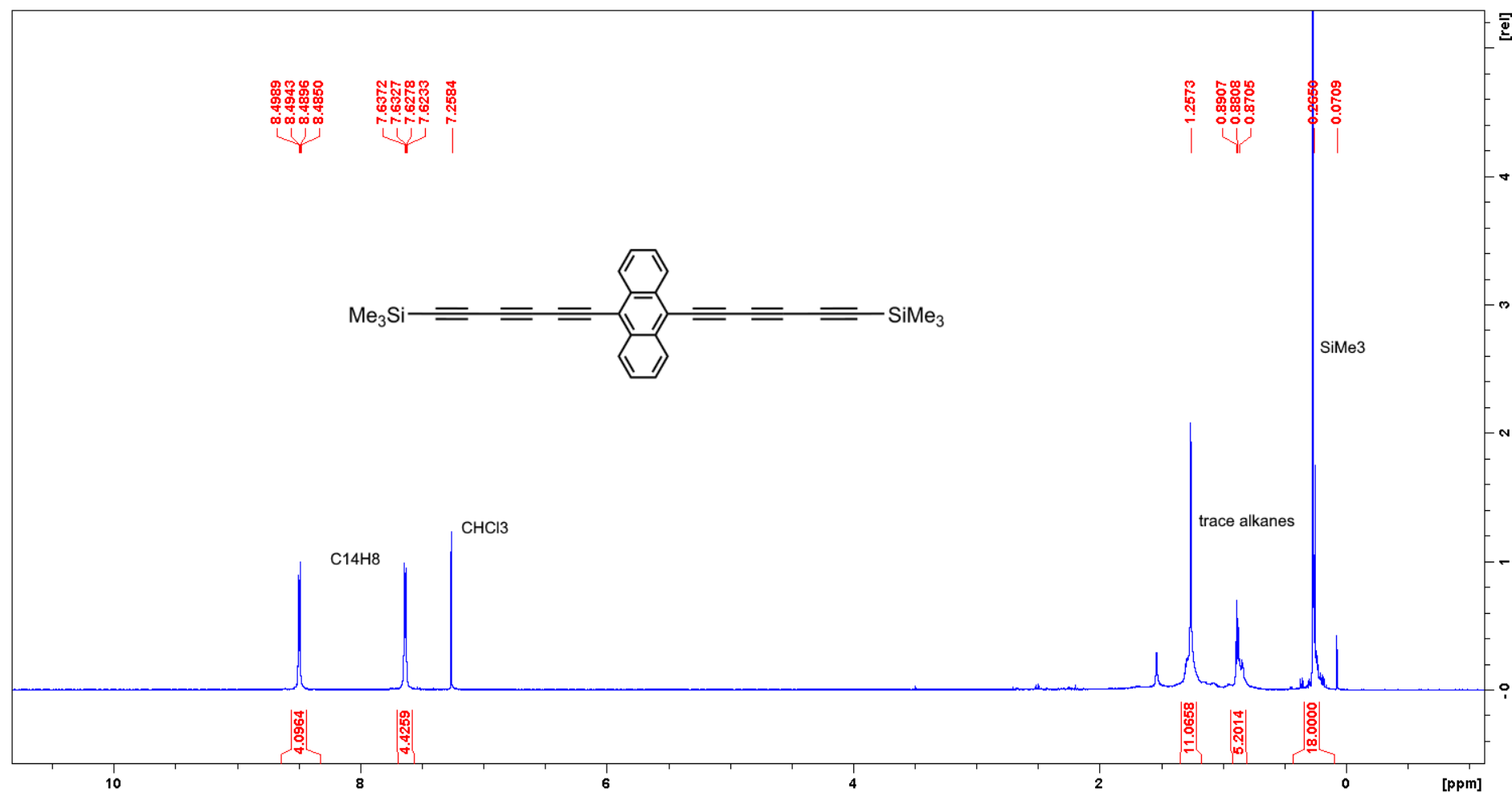


Figure S19. ^1H NMR (700 MHz, CDCl₃, 25°C, δ) of 9,10-bis(trimethylsilyl)hexa-1,3,5-triyn-1-yl)anthracene (**10**).

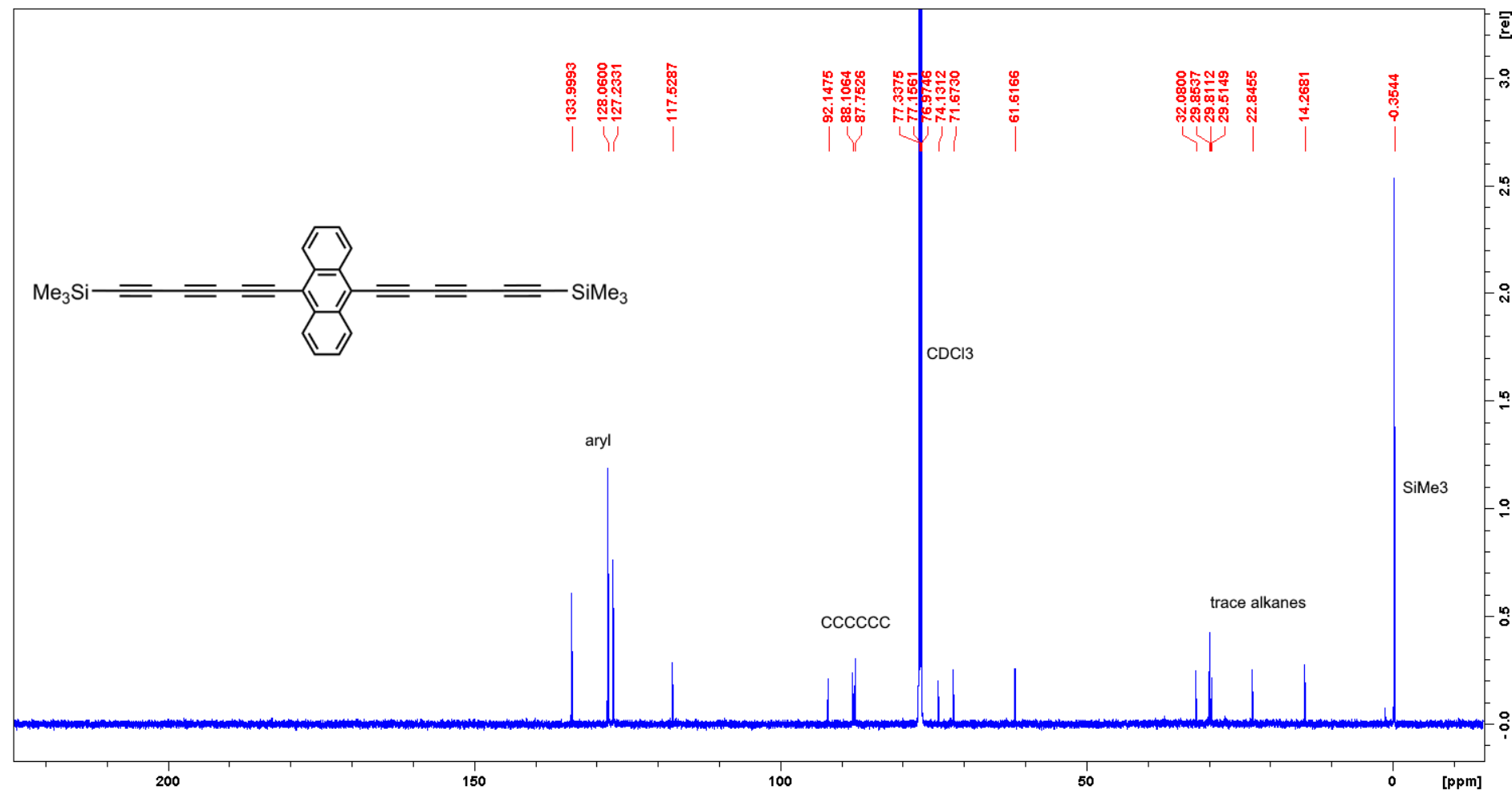


Figure S20. $^{13}\text{C}\{^1\text{H}\}$ NMR (176 MHz, CDCl_3 , 25°C, δ) of 9,10-bis(trimethylsilyl)hexa-1,3,5-triyn-1-yl)anthracene (**10**).

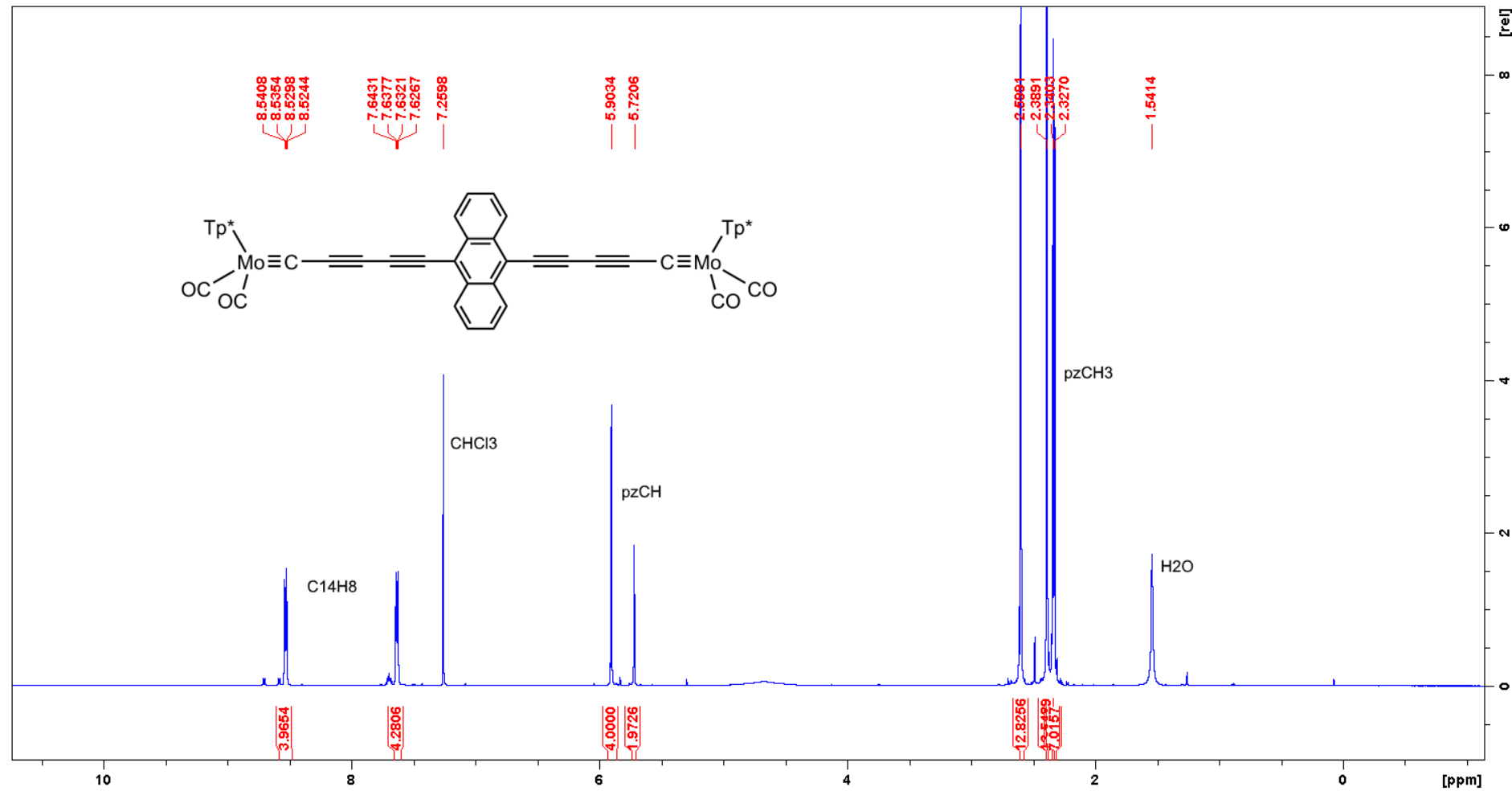


Figure S21. ^1H NMR (700 MHz, CDCl_3 , 25°C , δ) of [9,10- $\{\text{Tp}^*\}(\text{CO})_2\text{Mo}\equiv\text{CC}\equiv\text{CC}\equiv\text{C}\}\text{C}_{14}\text{H}_8$] (11).

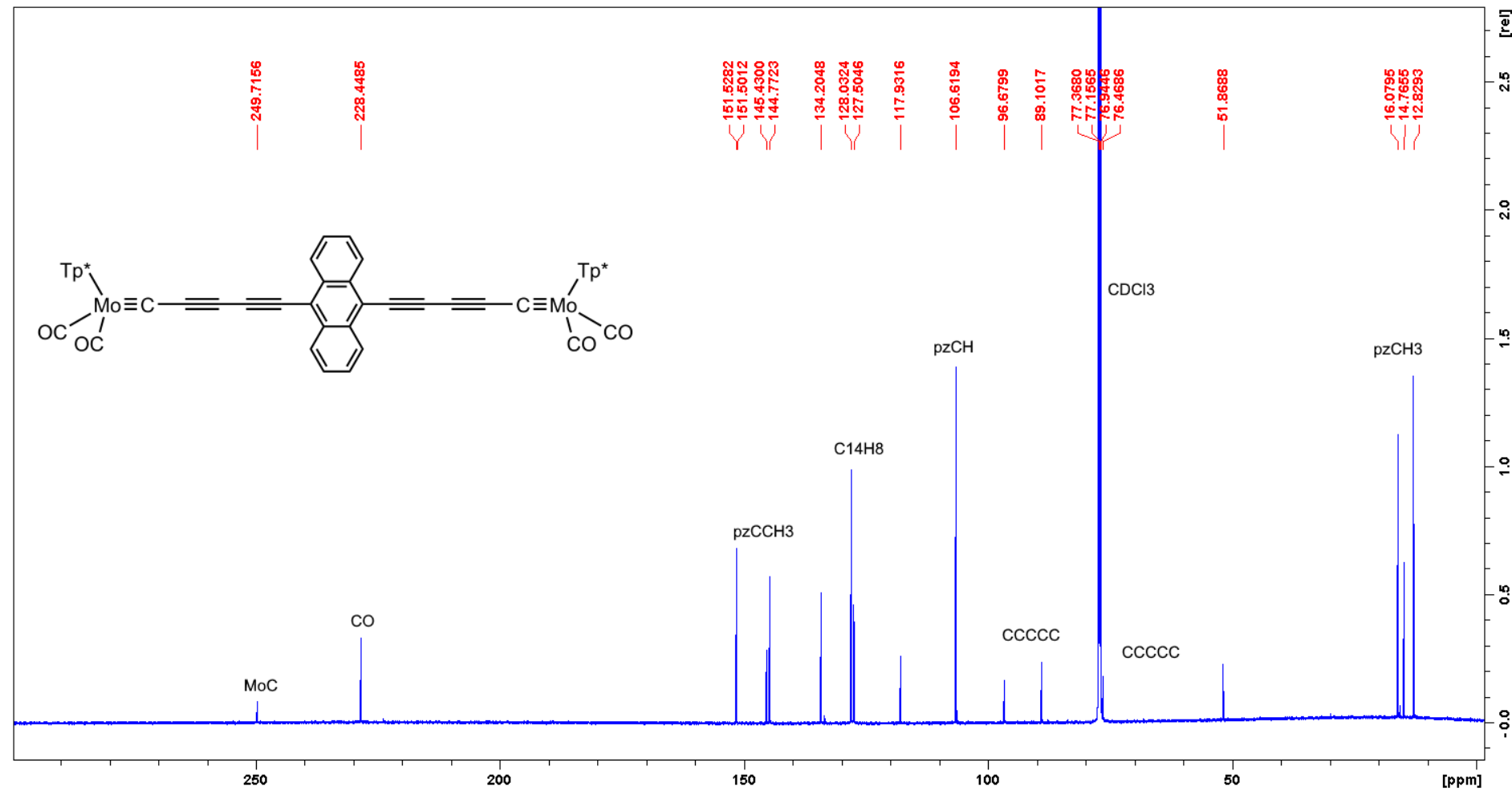


Figure S22. $^{13}\text{C}\{^1\text{H}\}$ NMR (176 MHz, CDCl₃, 25 °C, δ) of [9,10- $\{(\text{Tp}^*)(\text{CO})_2\text{Mo}\equiv\text{CC}\equiv\text{CC}\equiv\text{C}\}\text{C}_{14}\text{H}_8$] (11).

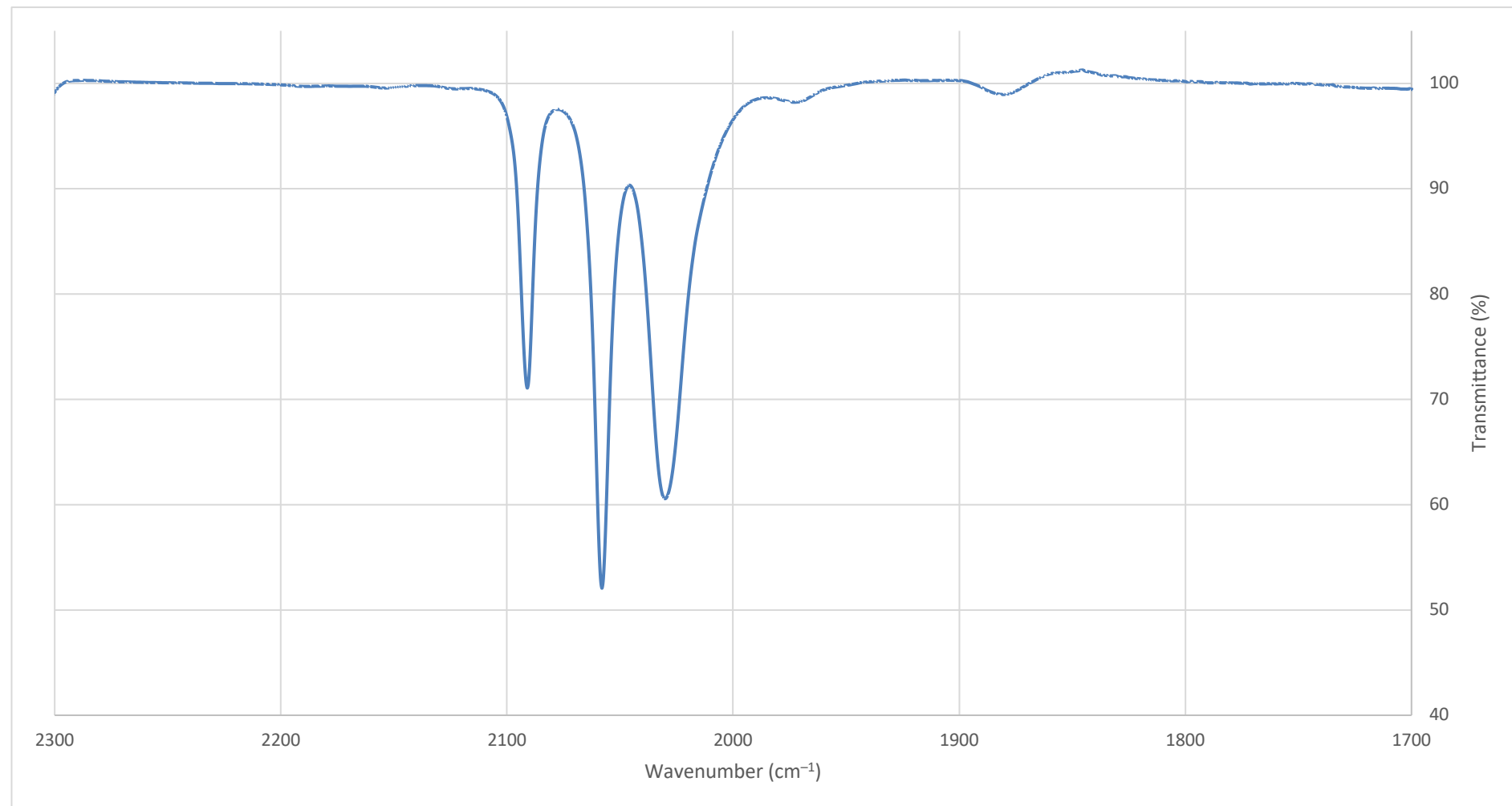


Figure S23. Infrared spectrum (CH_2Cl_2 , cm^{-1}) of the tetracobalt complex **5**.

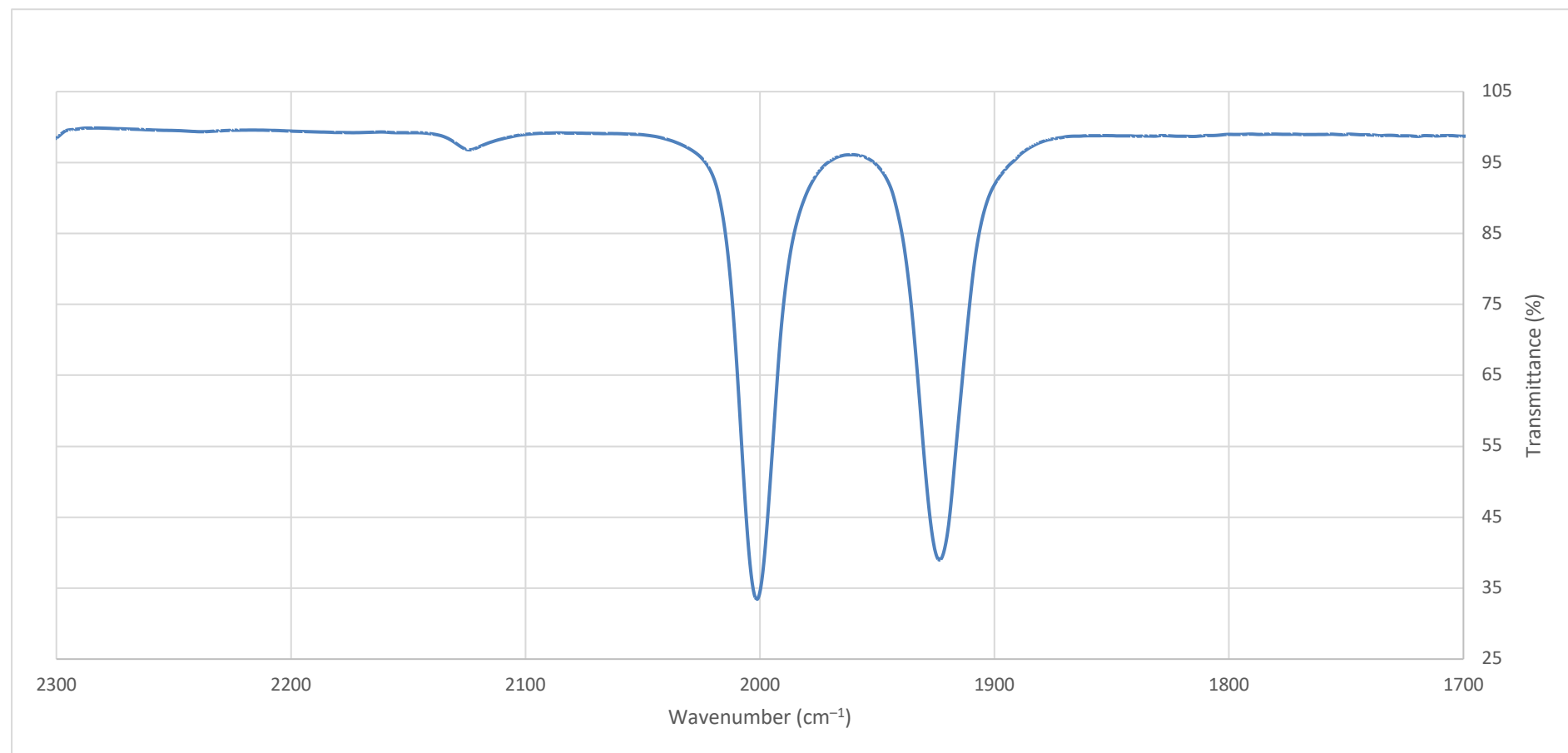


Figure S24. Infrared spectrum (CH_2Cl_2 , cm^{-1}) of [9,10- $\{(Tp^*)(\text{CO})_2\text{Mo}\equiv\text{CC}\equiv\text{CC}\equiv\text{C}\}\text{C}_{14}\text{H}_8$] (**11**).

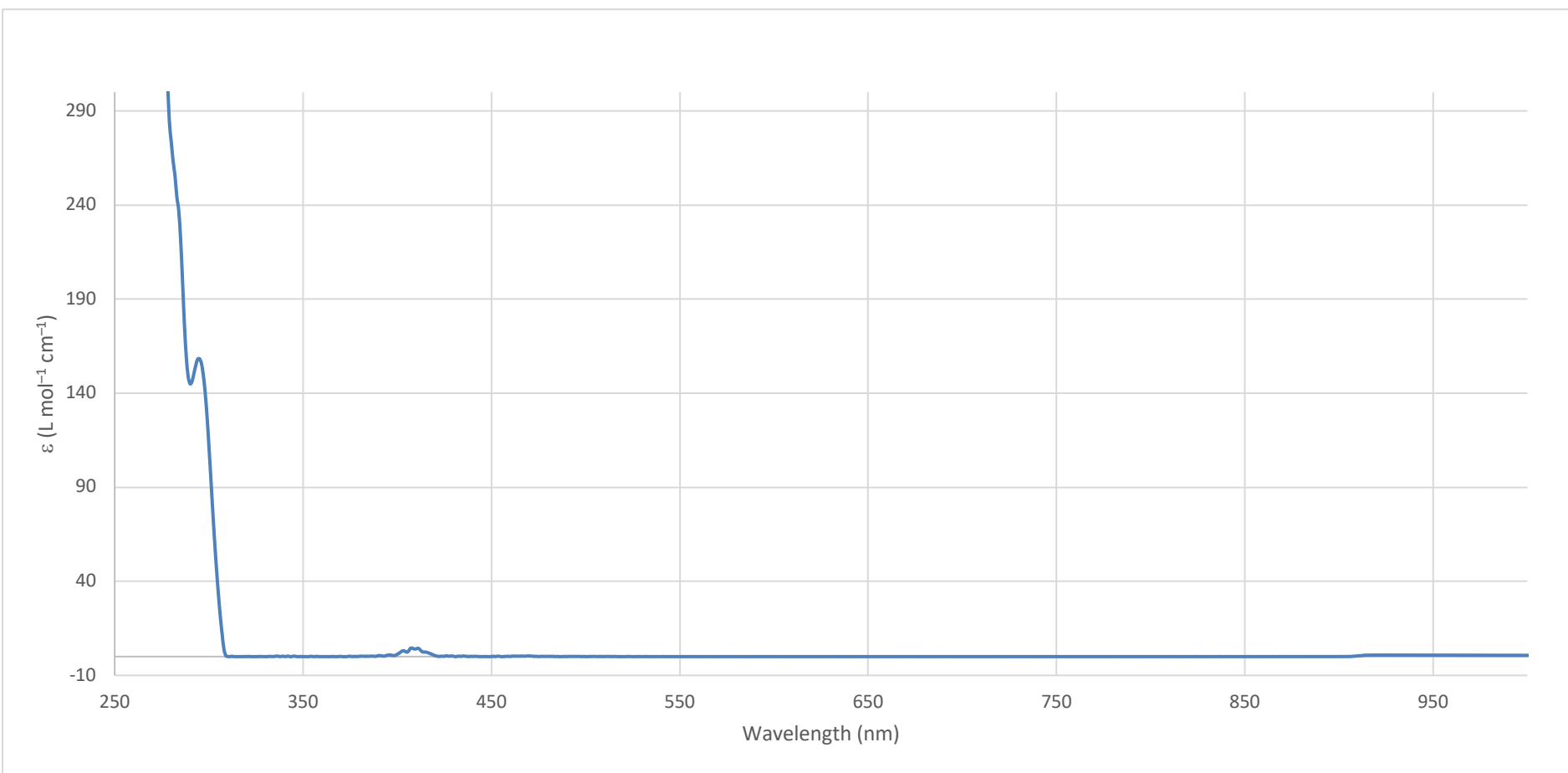


Figure S25. Electronic spectrum (CH_2Cl_2) of *anti*-9,10-dimethoxy-9,10-bis(trimethylsilylbut-1,3-diyen-1-yl)dihydroanthracene (**2**).

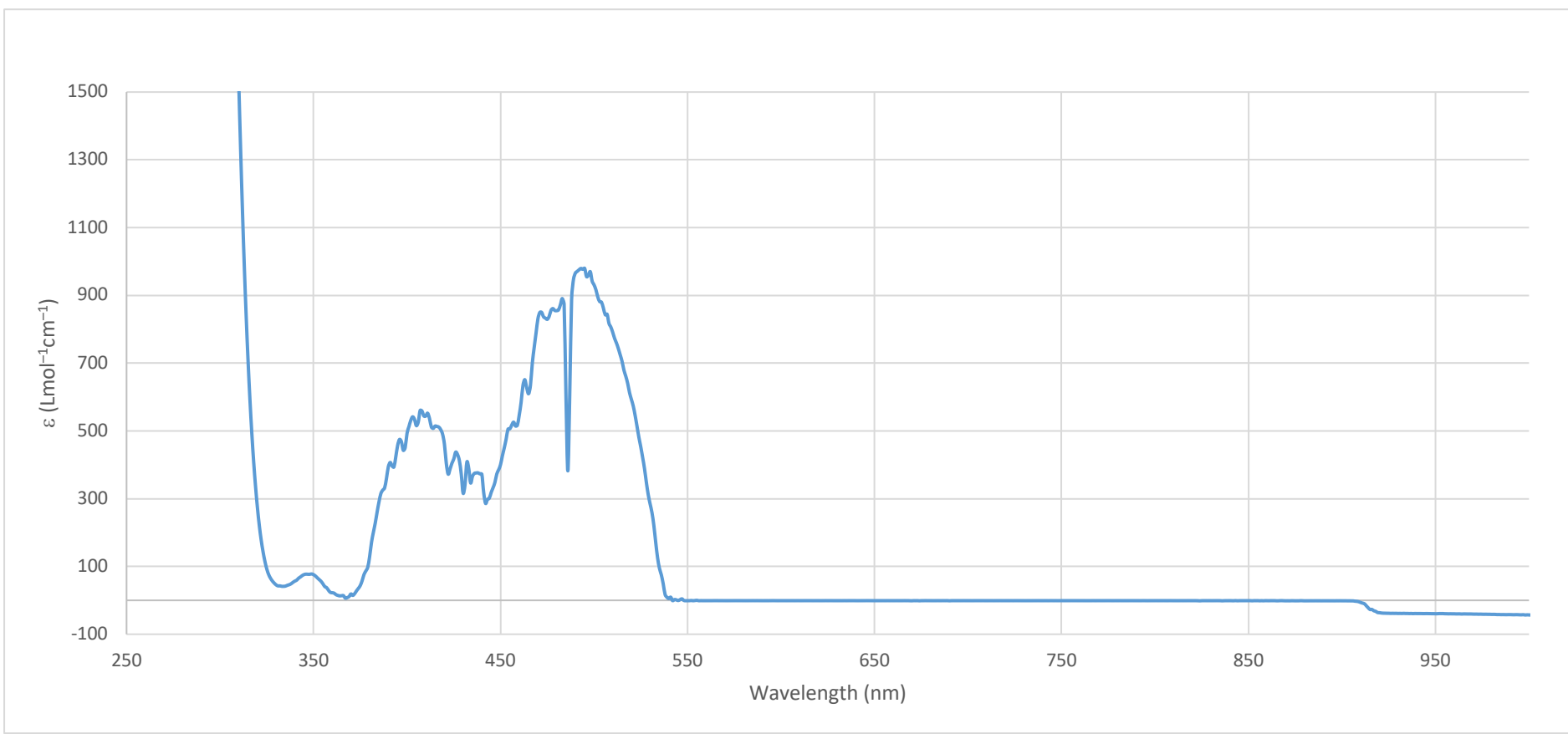


Figure S26. Electronic spectrum (CH_2Cl_2) of 10-hydroxy-10-(trimethylsilylbuta-1,3-diyne-1-yl)anthracen-9(10H)-one (**3**).

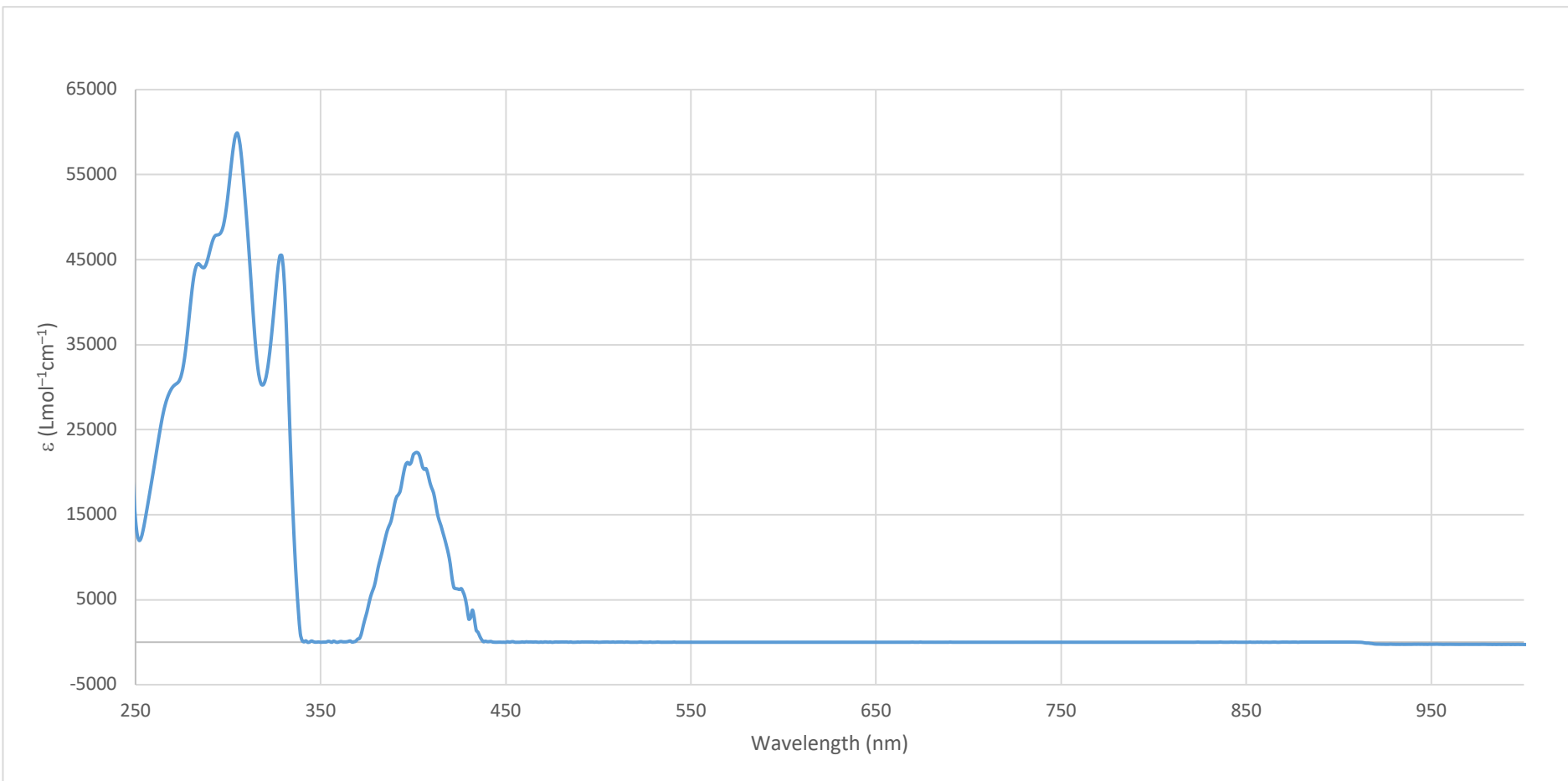


Figure S27. Electronic spectrum (CH_2Cl_2) of dimerization product (4).

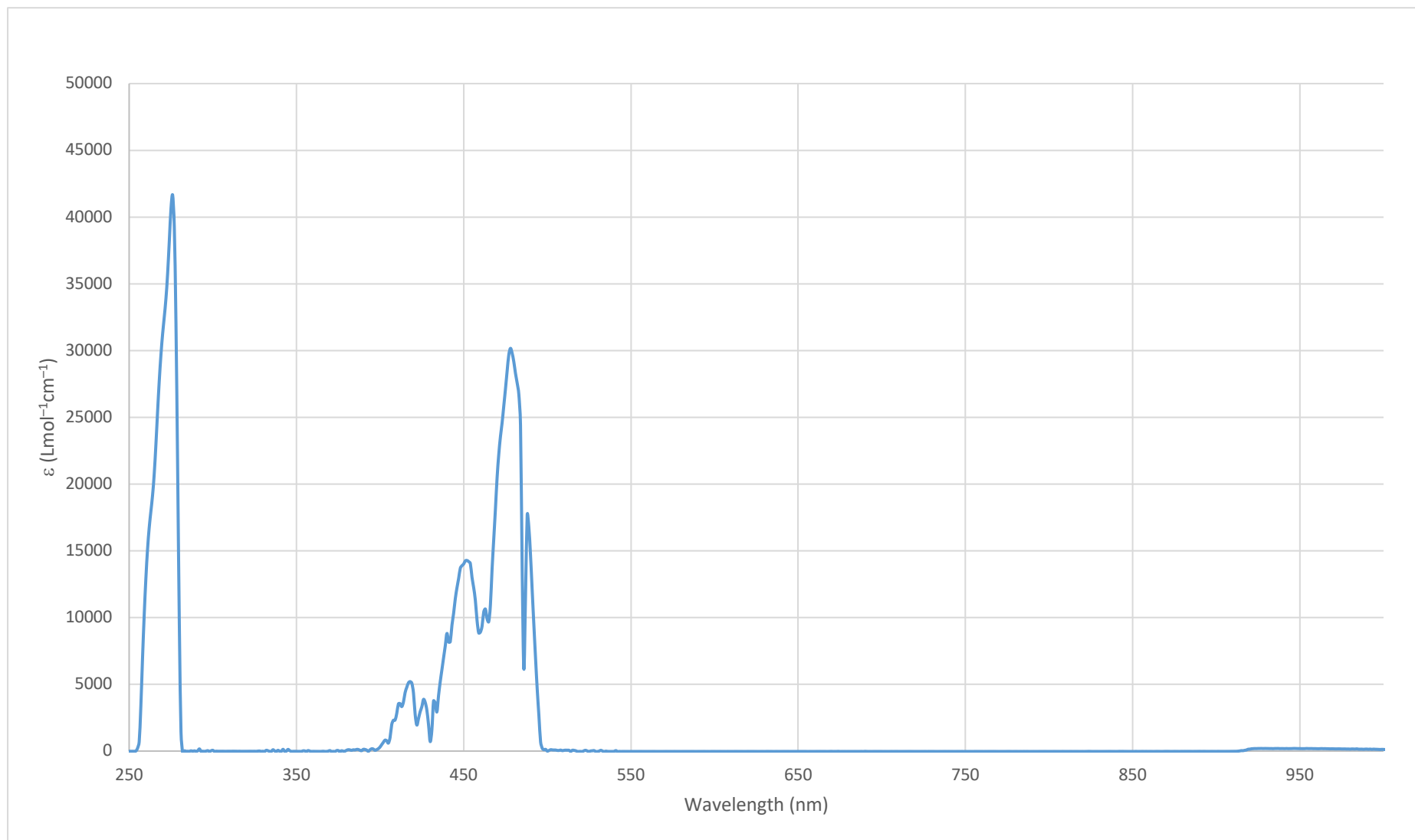


Figure S28. Electronic spectrum (CH_2Cl_2) of 9,10-bis(phenylbut-1,3-diyn-1-yl)anthracene (5).

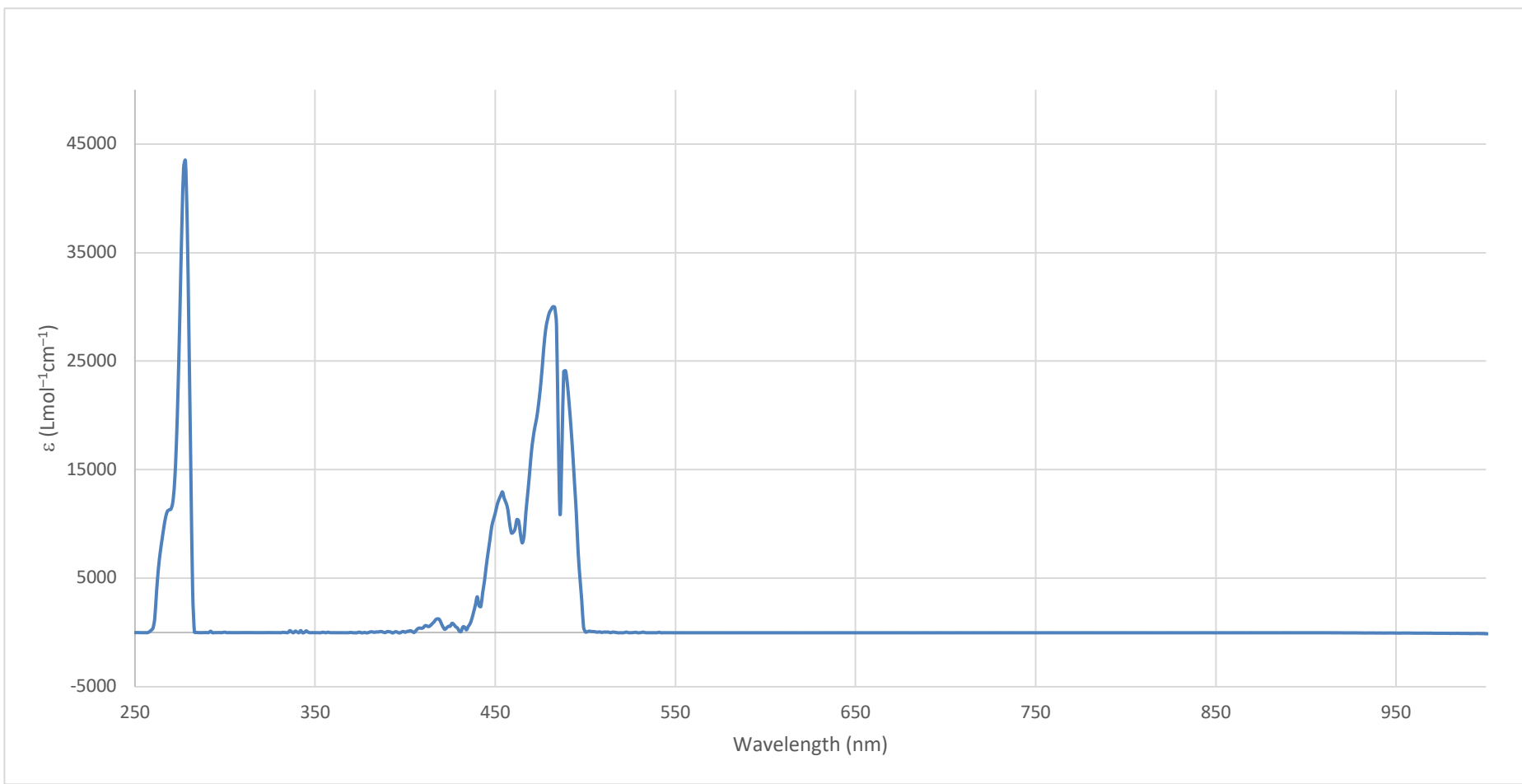


Figure S29. Electronic spectrum (CH_2Cl_2) of 9,10-bis((4-bromophenyl)but-1,3-diyne-1-yl)anthracene (**6**).

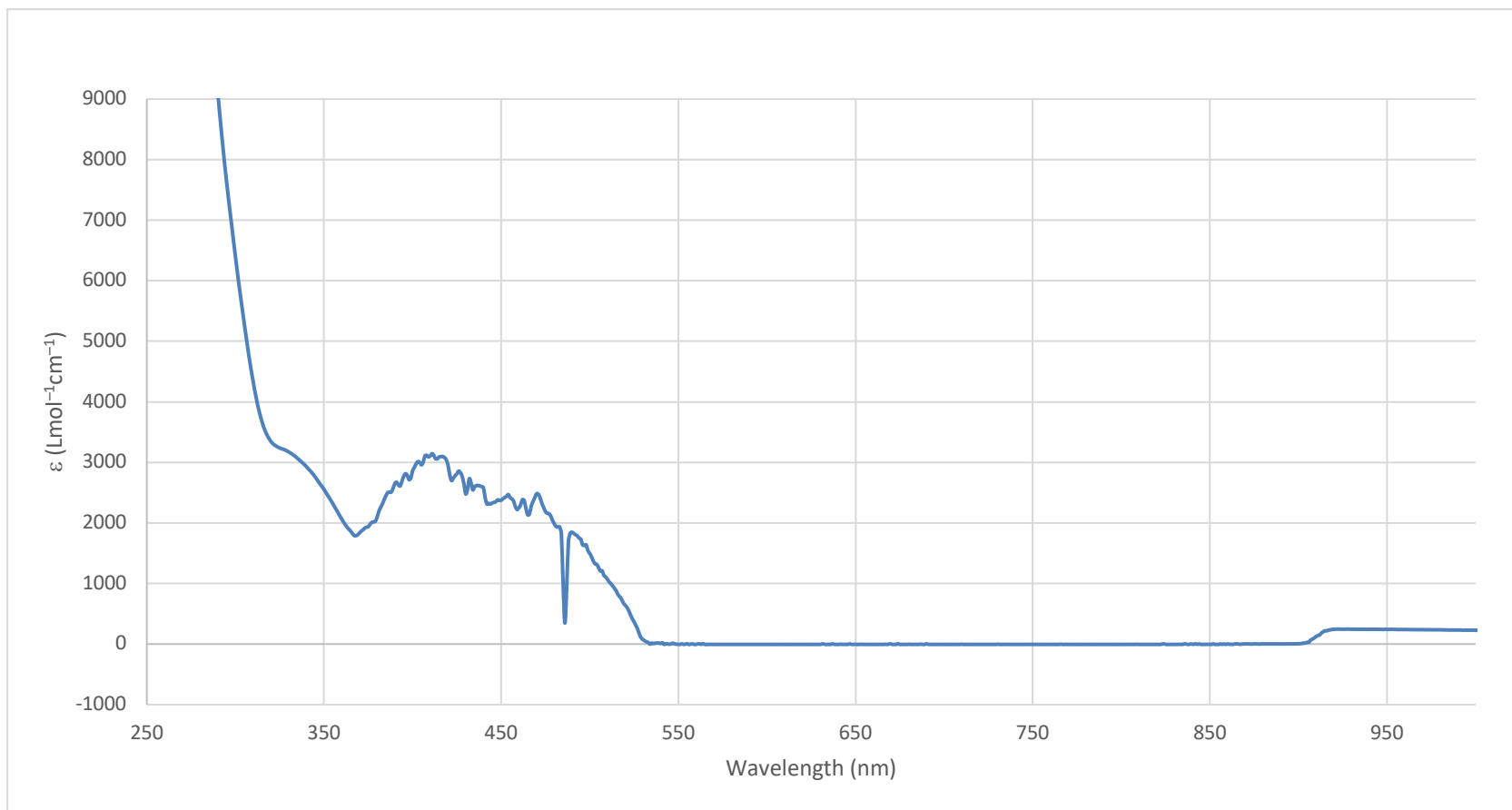


Figure S30. Electronic spectrum (CH_2Cl_2) of tetracobalt complex (7).

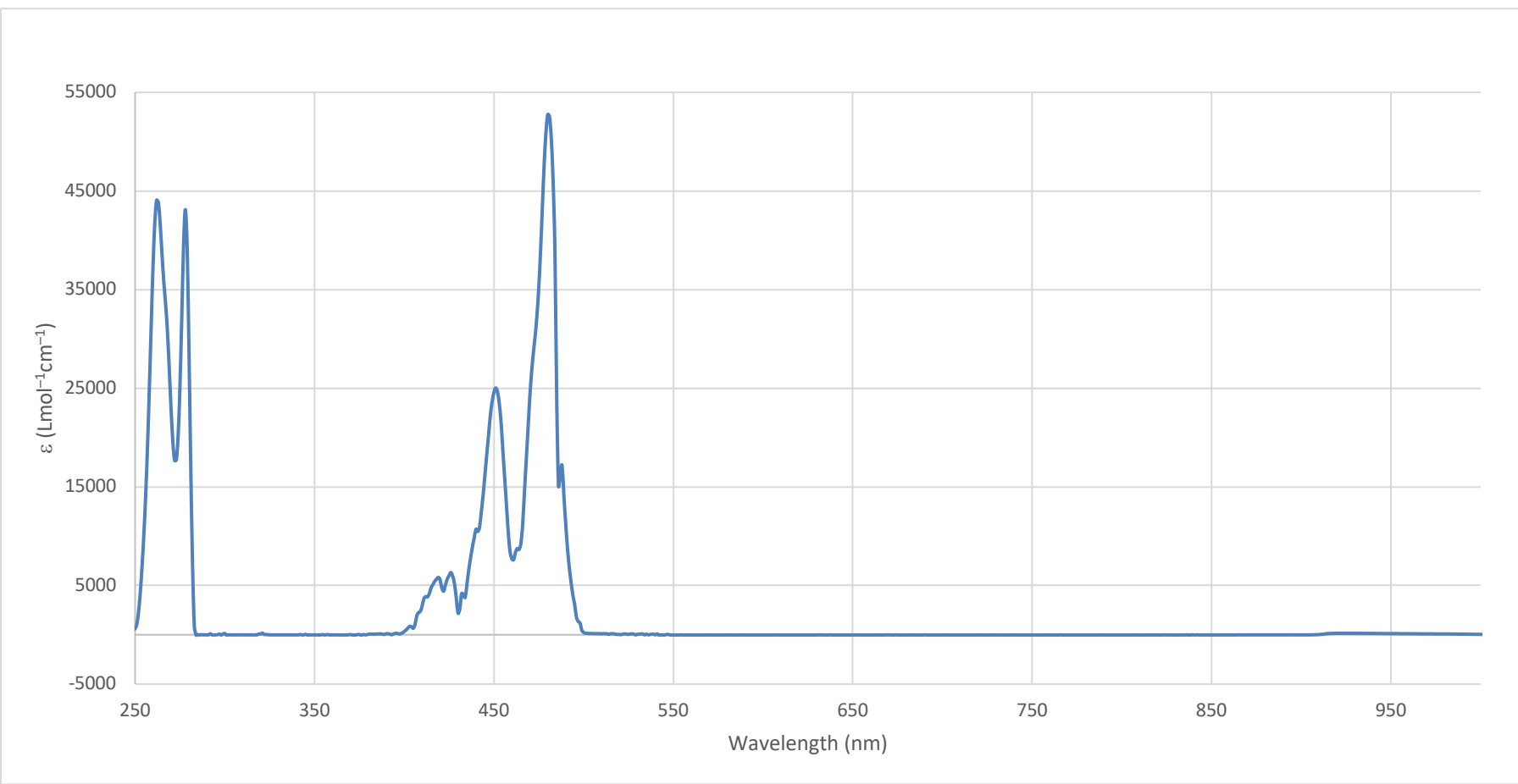


Figure S31. Electronic spectrum (CH_2Cl_2) of 9,10-bis(triphenylphosphinegold-but-1,3-diyn-1-yl)anthracene (**8**).

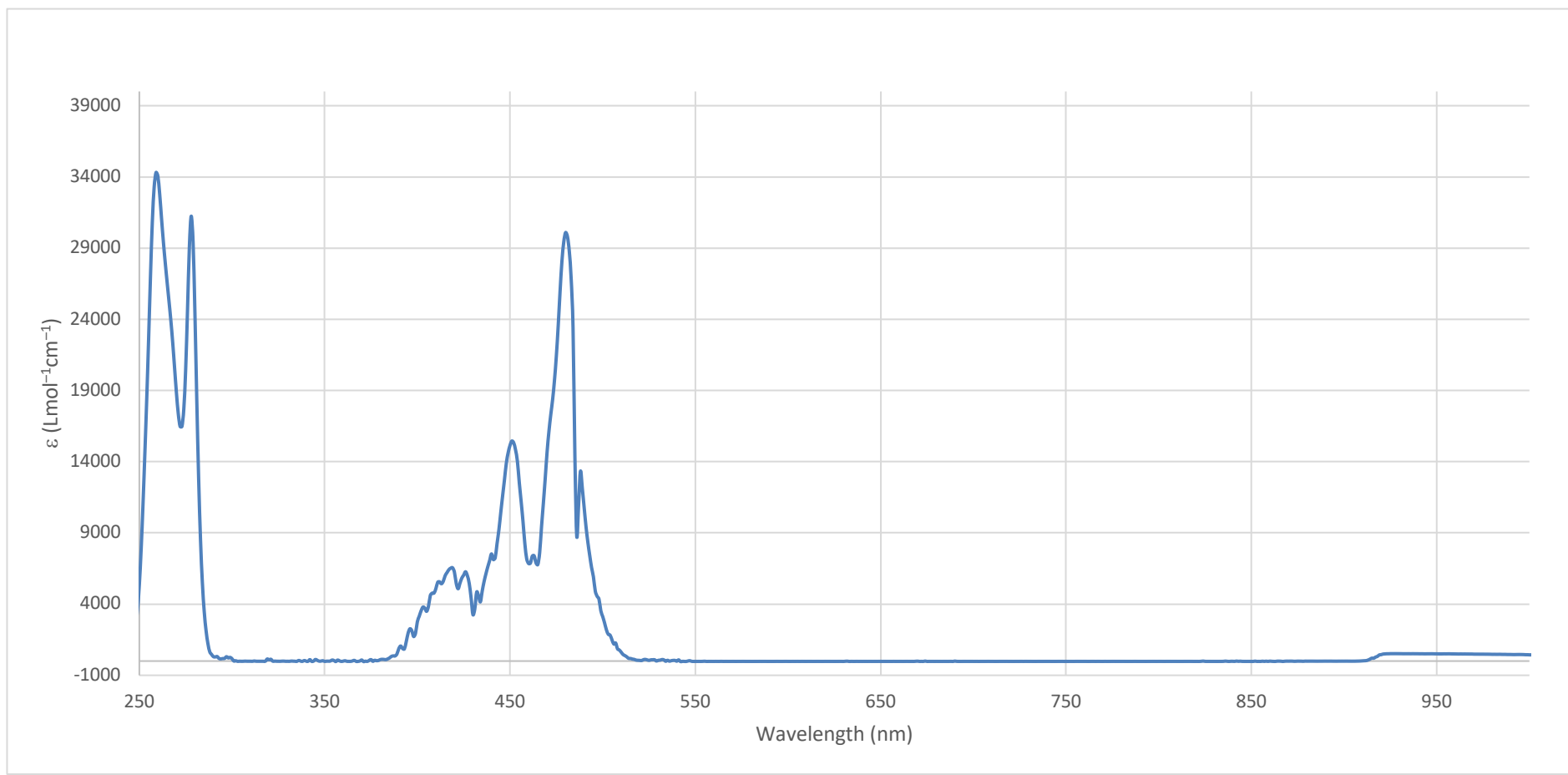


Figure S32. Electronic spectrum (CH_2Cl_2) of 9,10-bis(tricyclohexylphosphinegold-but-1,3-diyn-1-yl)anthracene (**9**).

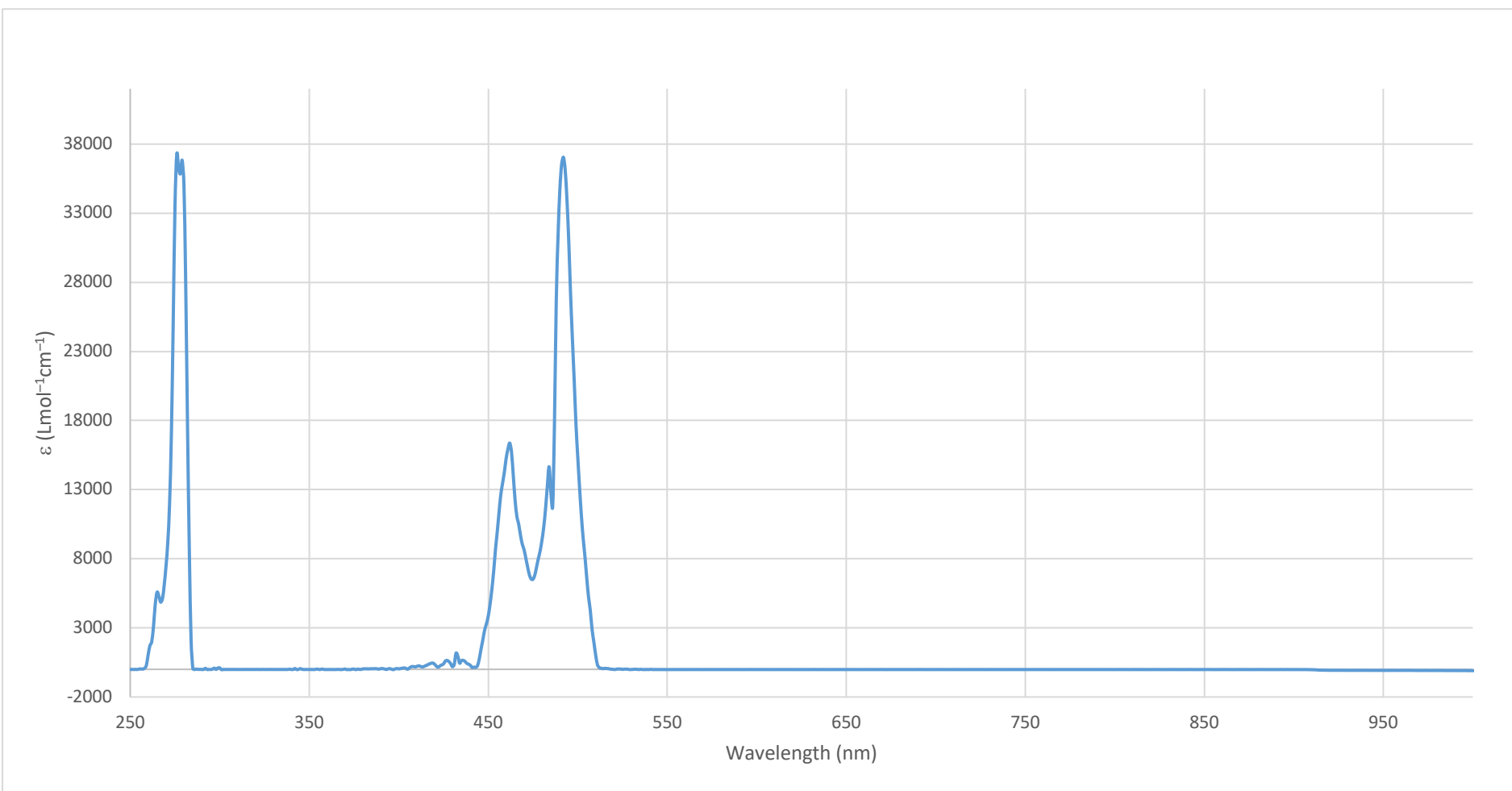


Figure S33. Electronic spectrum (CH_2Cl_2) of 9,10-bis((trimethylsilyl)hexa-1,3,5-triyn-1-yl)anthracene (**10**).

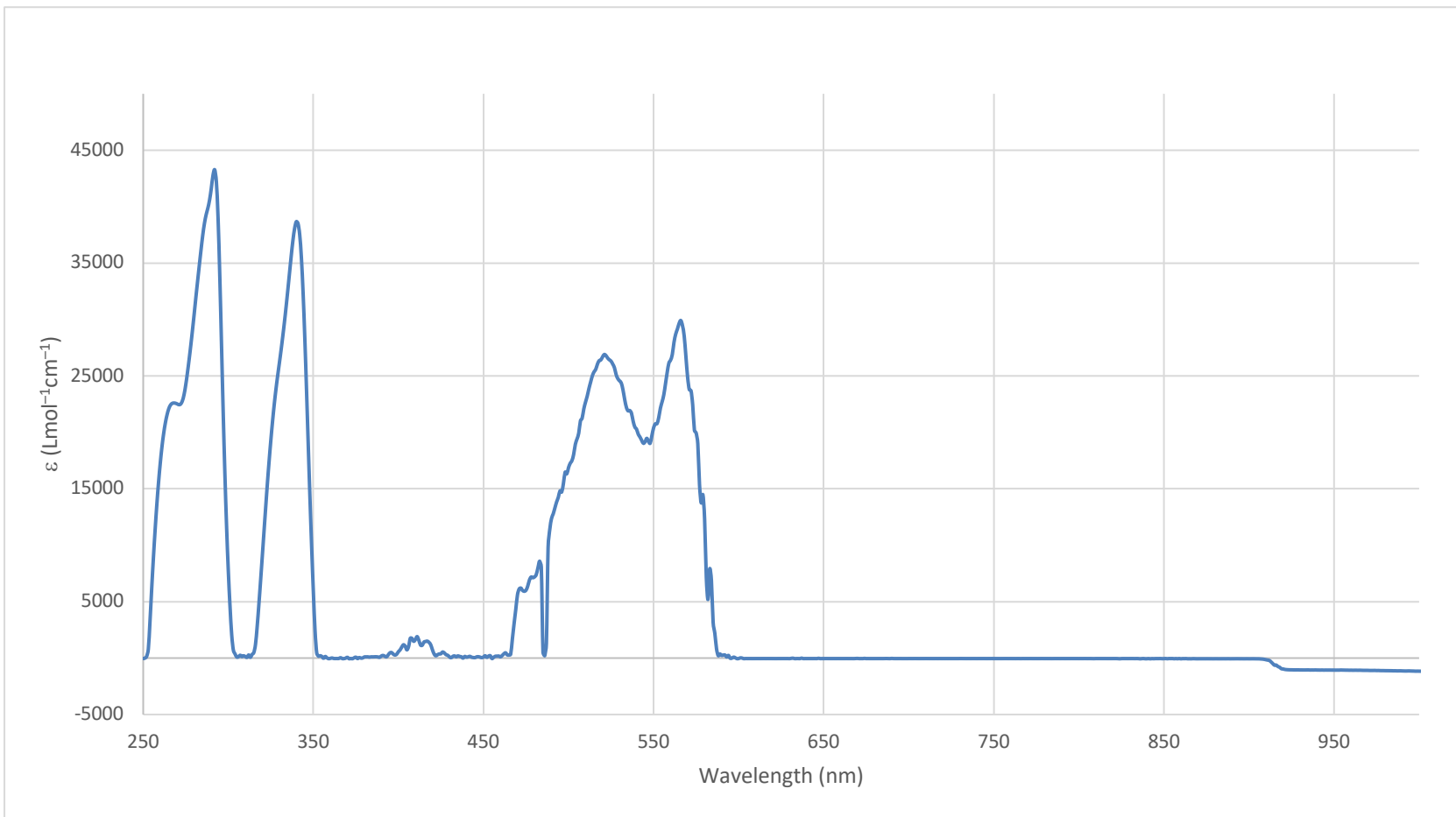


Figure S34. Electronic spectrum (CH_2Cl_2) of [9,10- $\{(\text{Tp}^*)(\text{CO})_2\text{Mo}\equiv\text{CC}\equiv\text{C}\}\text{C}_{14}\text{H}_8$] (11).

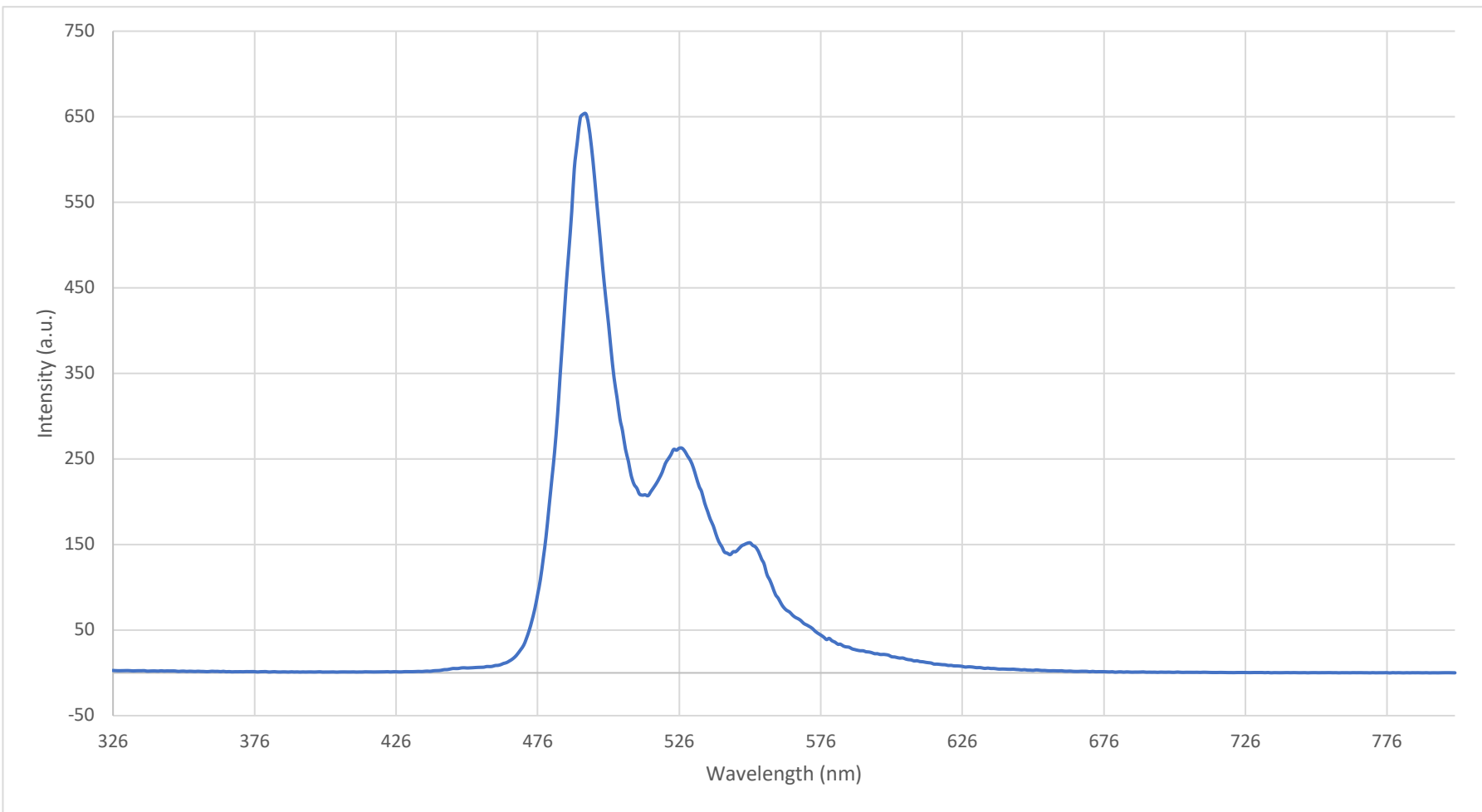


Figure S35. Emission spectrum (CH_2Cl_2) of 9,10-bis(phenylbut-1,3-diyn-1-yl)anthracene (**5**) with 276 nm excitation.

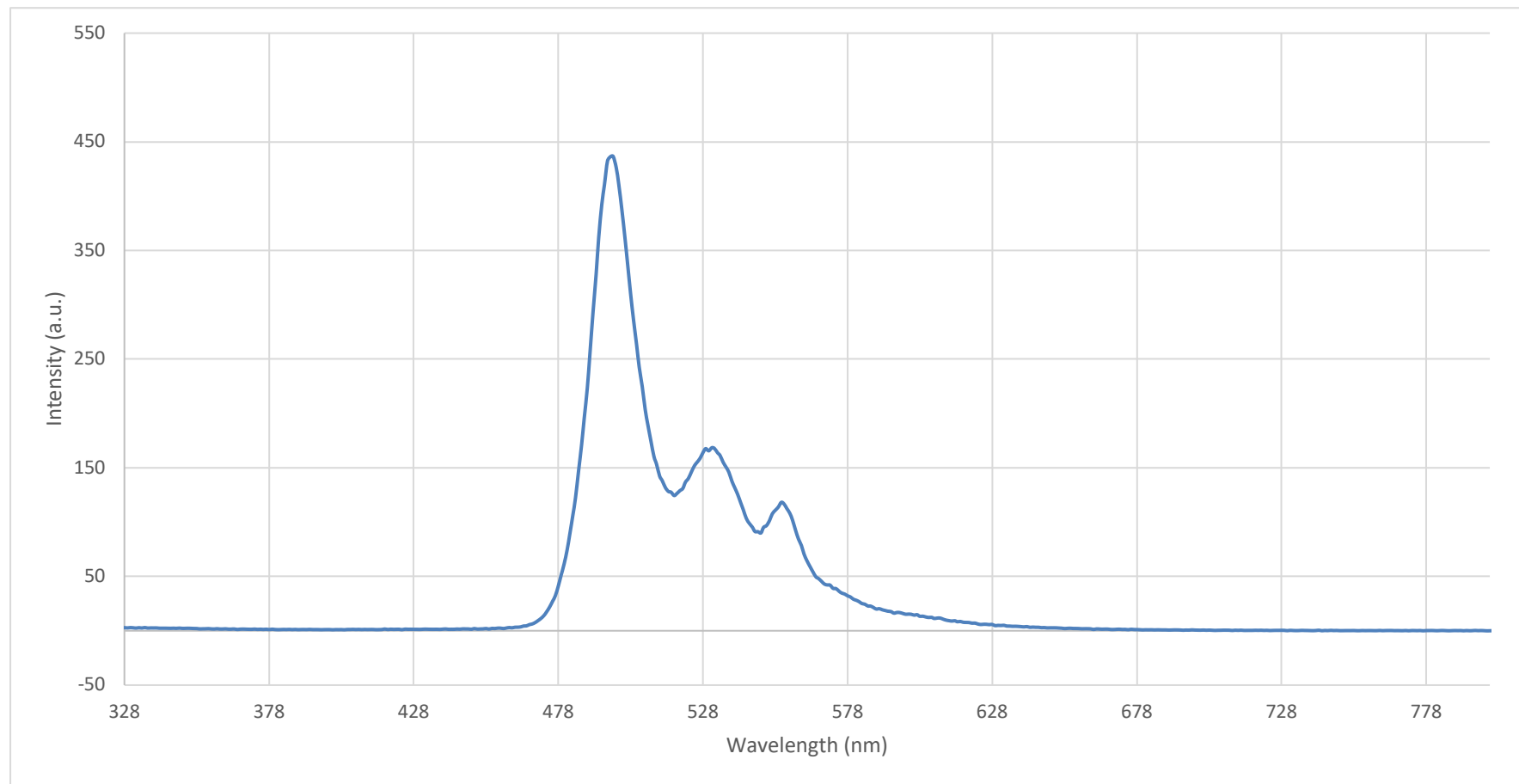


Figure S36. Emission spectrum (CH_2Cl_2) of 9,10-bis((4-bromophenyl)but-1,3-diyne-1-yl)anthracene (**6**) with 278 nm excitation.

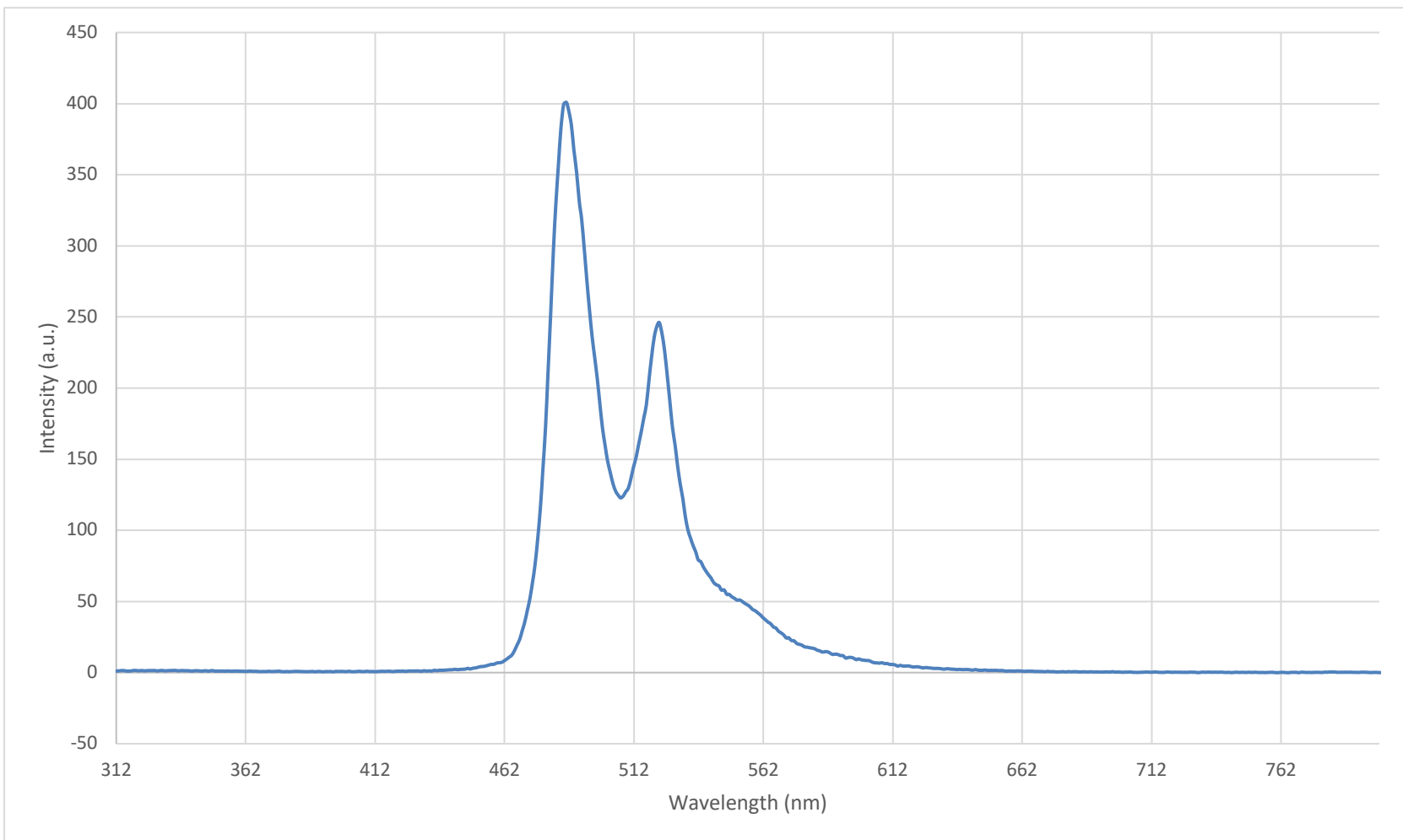


Figure S37. Emission spectrum (CH_2Cl_2) of 9,10-bis(triphenylphosphinegold-buta-1,3-diyen-1-yl)anthracene (**8**) with 262 nm excitation.

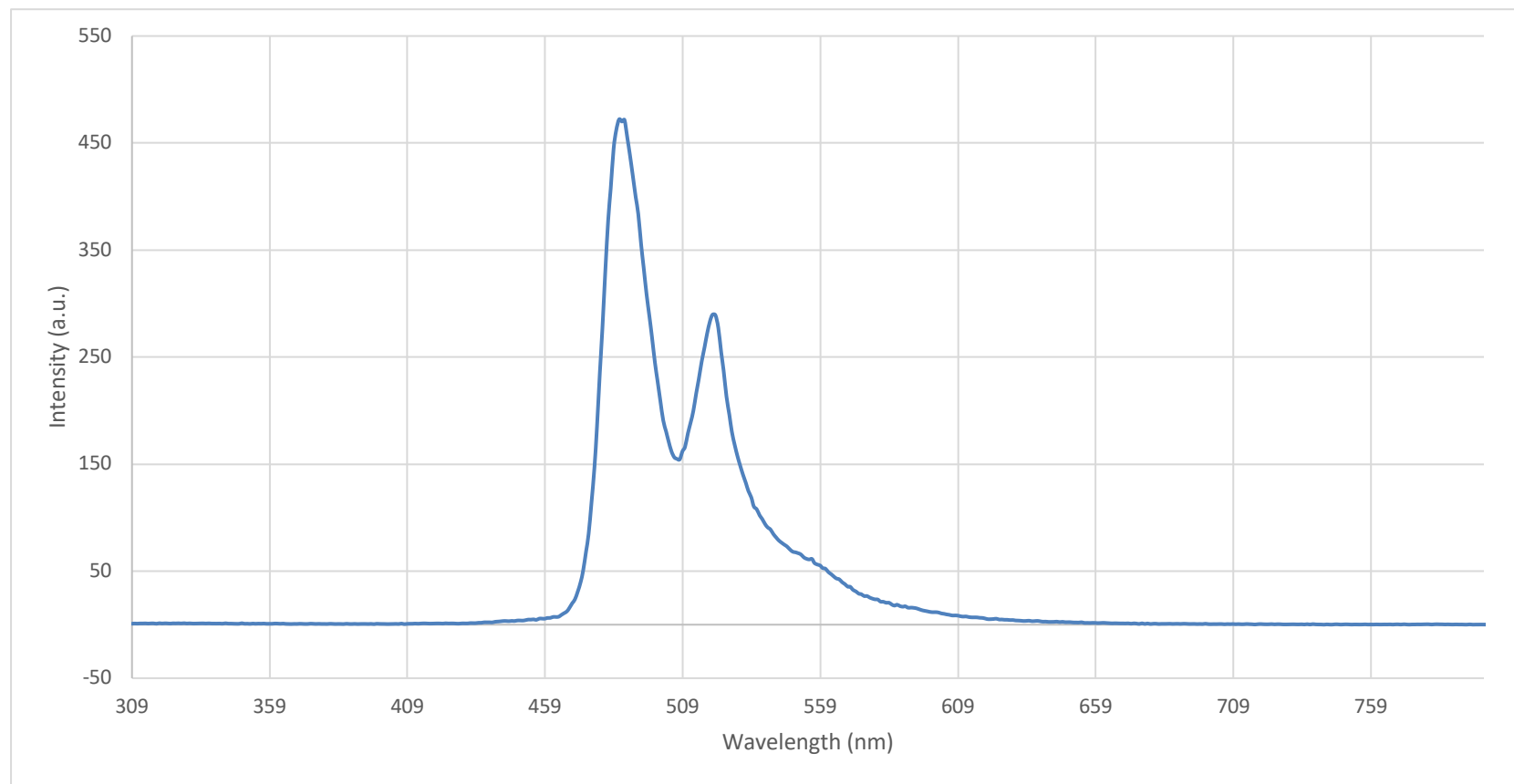


Figure S38. Emission spectrum (CH_2Cl_2) of 9,10-bis(tricyclohexylphosphinegold-buta-1,3-diyne-1-yl)anthracene (**9**) with 259 nm excitation.

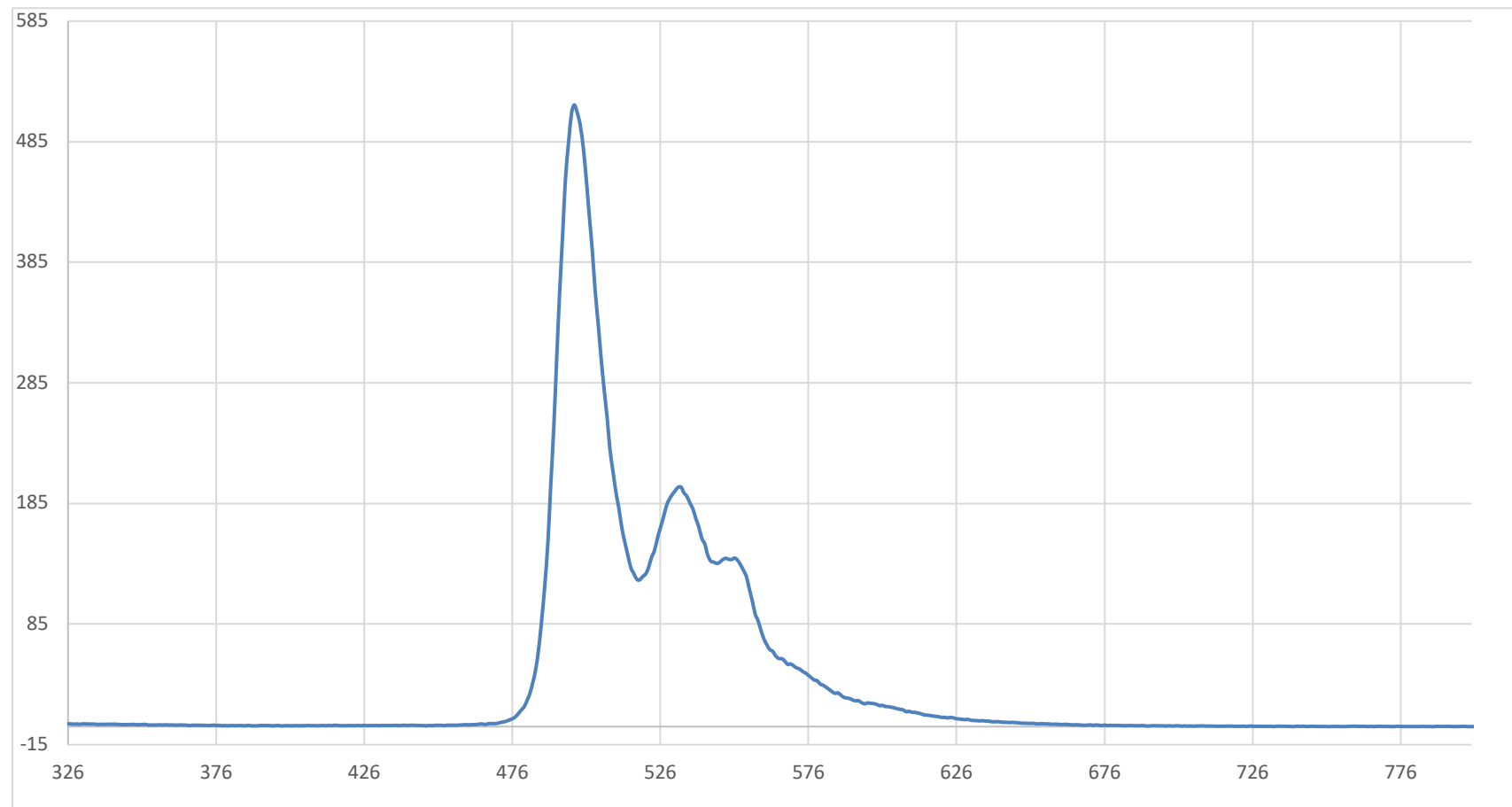


Figure S39. Emission spectrum (CH_2Cl_2) of 9,10-bis(trimethylsilyl)hexa-1,3,5-triyn-1-ylanthracene (**10**) with 276 nm excitation.

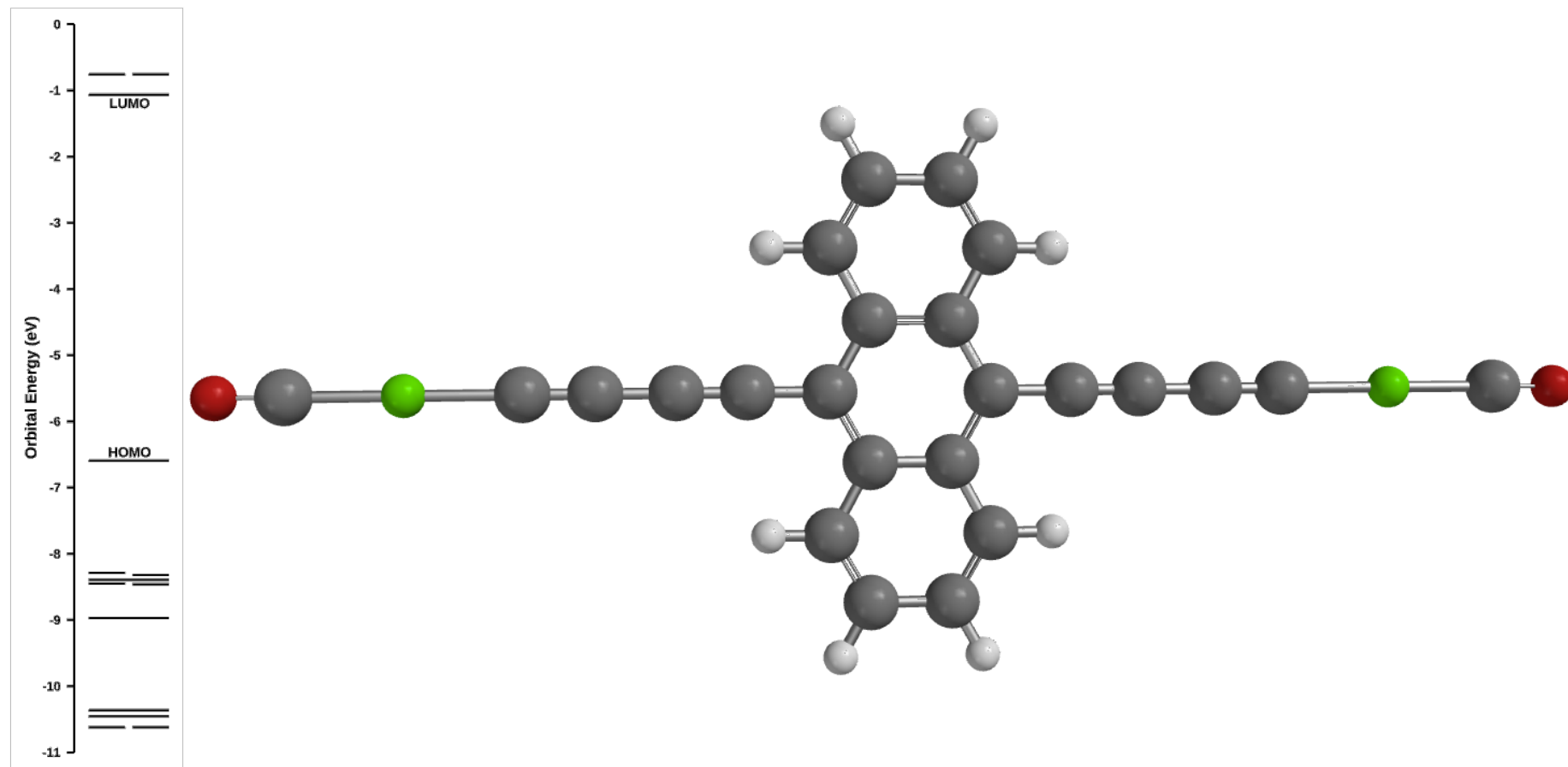


Figure S40. Optimised Geometry and frontier orbitals of $(\text{OC})\text{Au}-\text{C}\equiv\text{C}-\text{C}\equiv\text{C}-\text{C}_{14}\text{H}_8-\text{C}\equiv\text{C}-\text{C}\equiv\text{C}-\text{Au}(\text{CO})$ ($\omega\text{B97X-D}/6-31\text{G}^*/\text{LANL2D}\zeta(\text{Au})/\text{Gas phase}$)

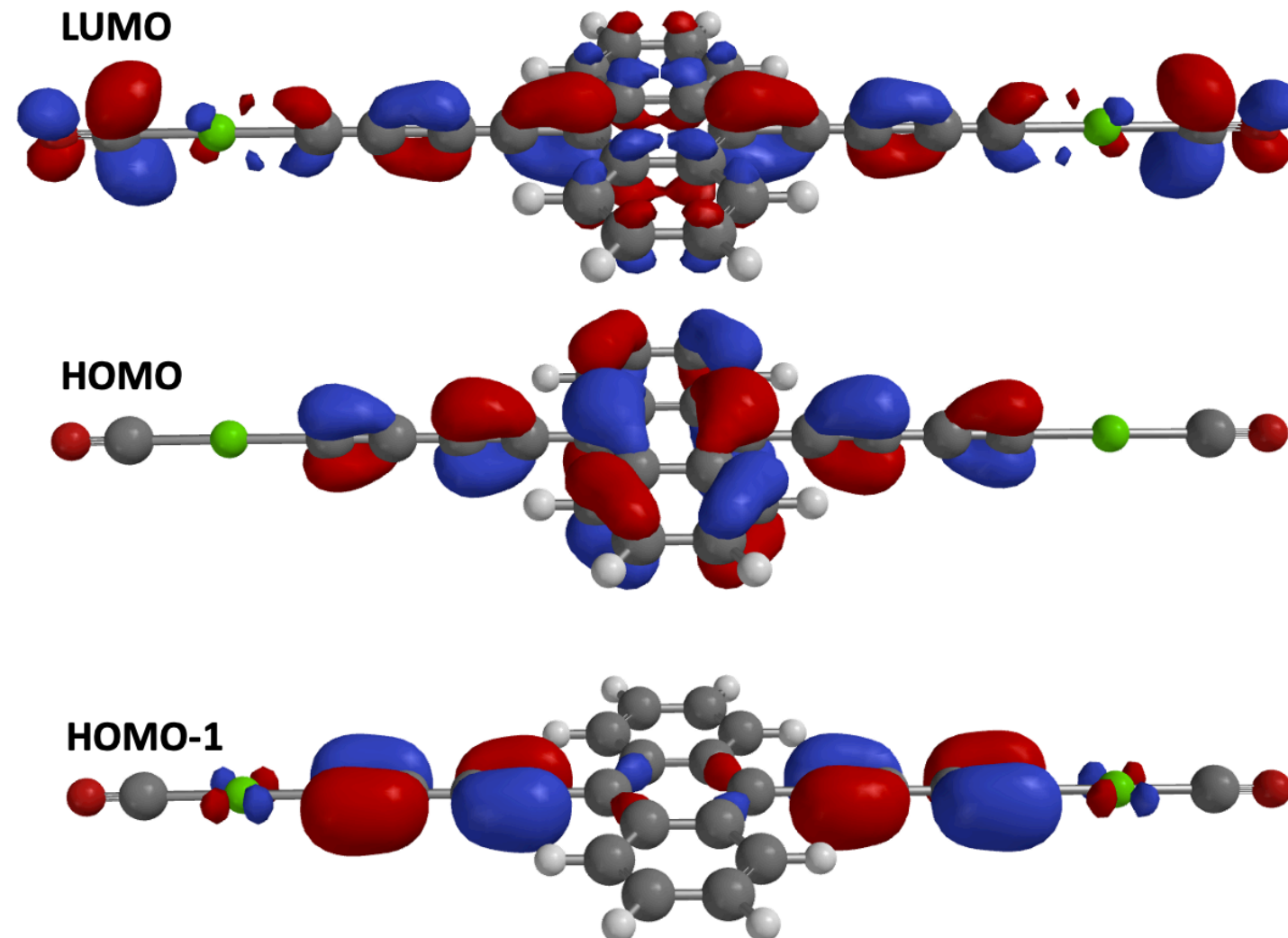


Figure S41. Frontier orbitals of interest for $(OC)Au-C\equiv C-C\equiv C-C_{14}H_8-C\equiv C-C\equiv C-Au(CO)$ (ω B97X-D/6-31G*/LANL2D ζ (Au)/Gas phase)

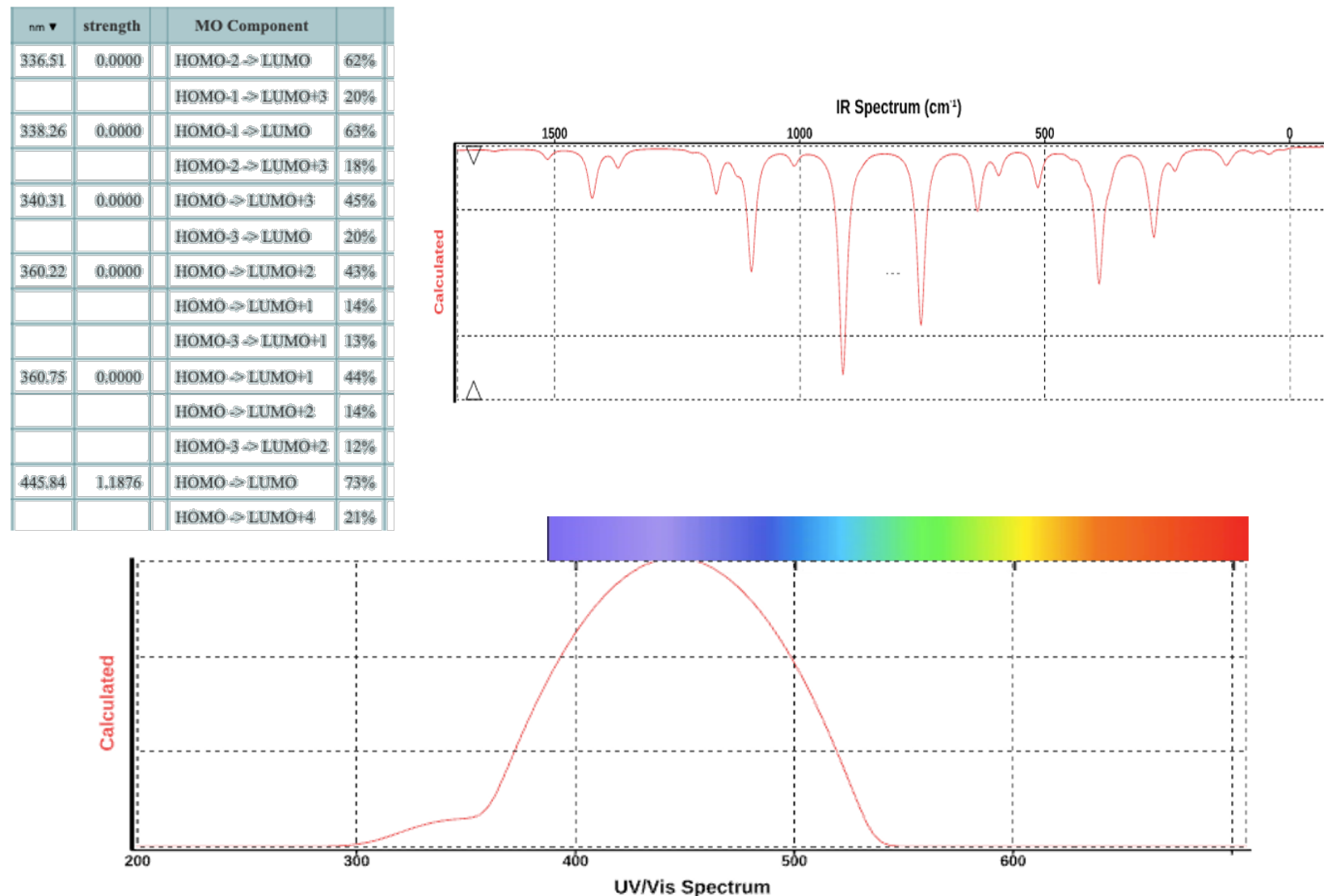


Figure S42. Calculated electronic and infrared spectra of (OC)Au-C≡C-C≡C-C₁₄H₈-C≡C-C≡C-Au(CO) (ωB97X-D/6-31G*/LANL2Dζ(Au)/Gas phase)

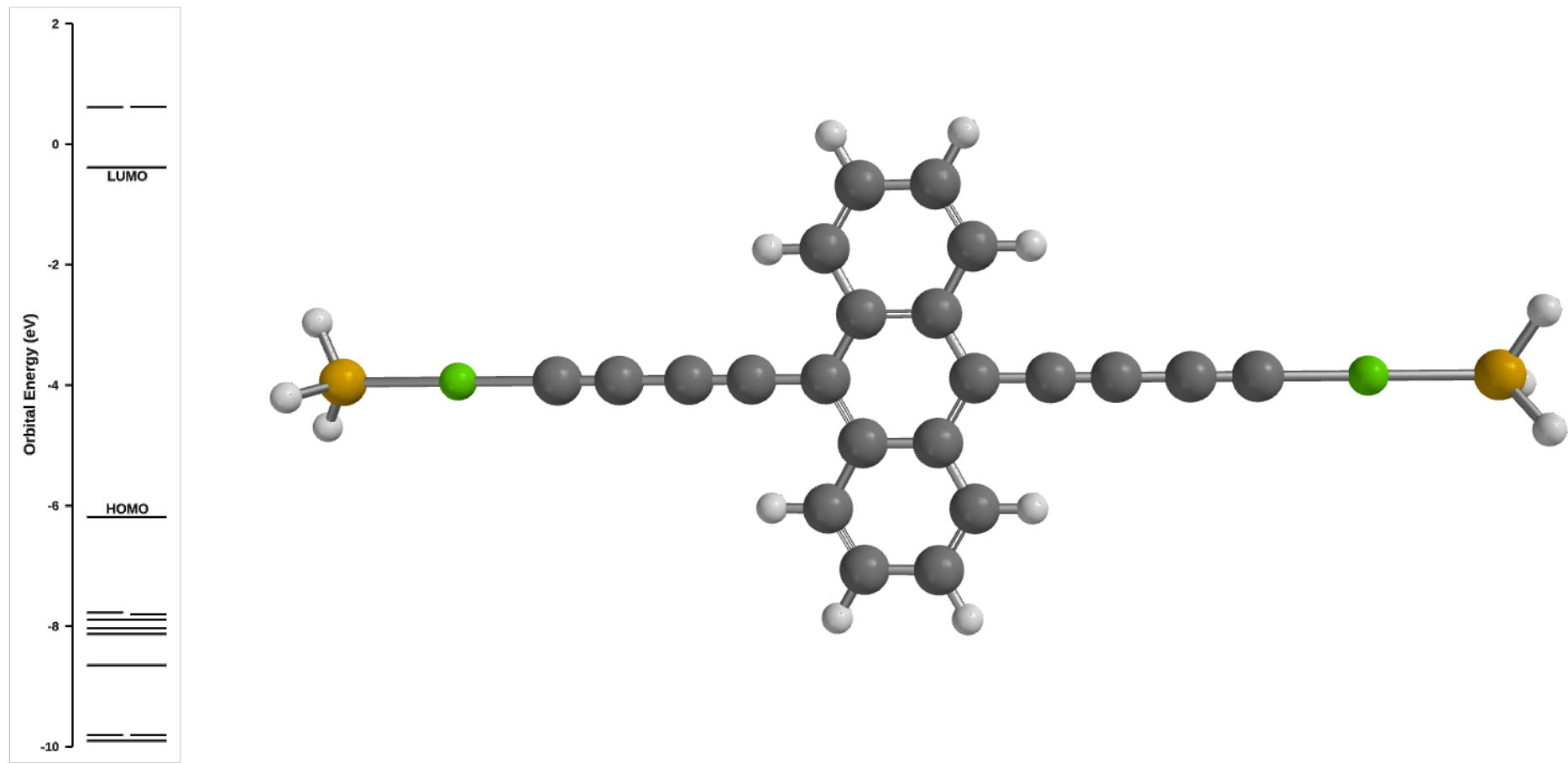


Figure S43. Optimised Geometry and frontier orbitals of $(\text{H}_3\text{P})\text{Au}-\text{C}=\text{C}-\text{C}-\text{C}_{14}\text{H}_8-\text{C}\equiv\text{C}-\text{C}\equiv\text{C}-\text{Au}(\text{PH}_3)$ ($\omega\text{B97X-D}/6-31\text{G}^*/\text{LANL2D}_5(\text{Au})/\text{Gas phase}$)

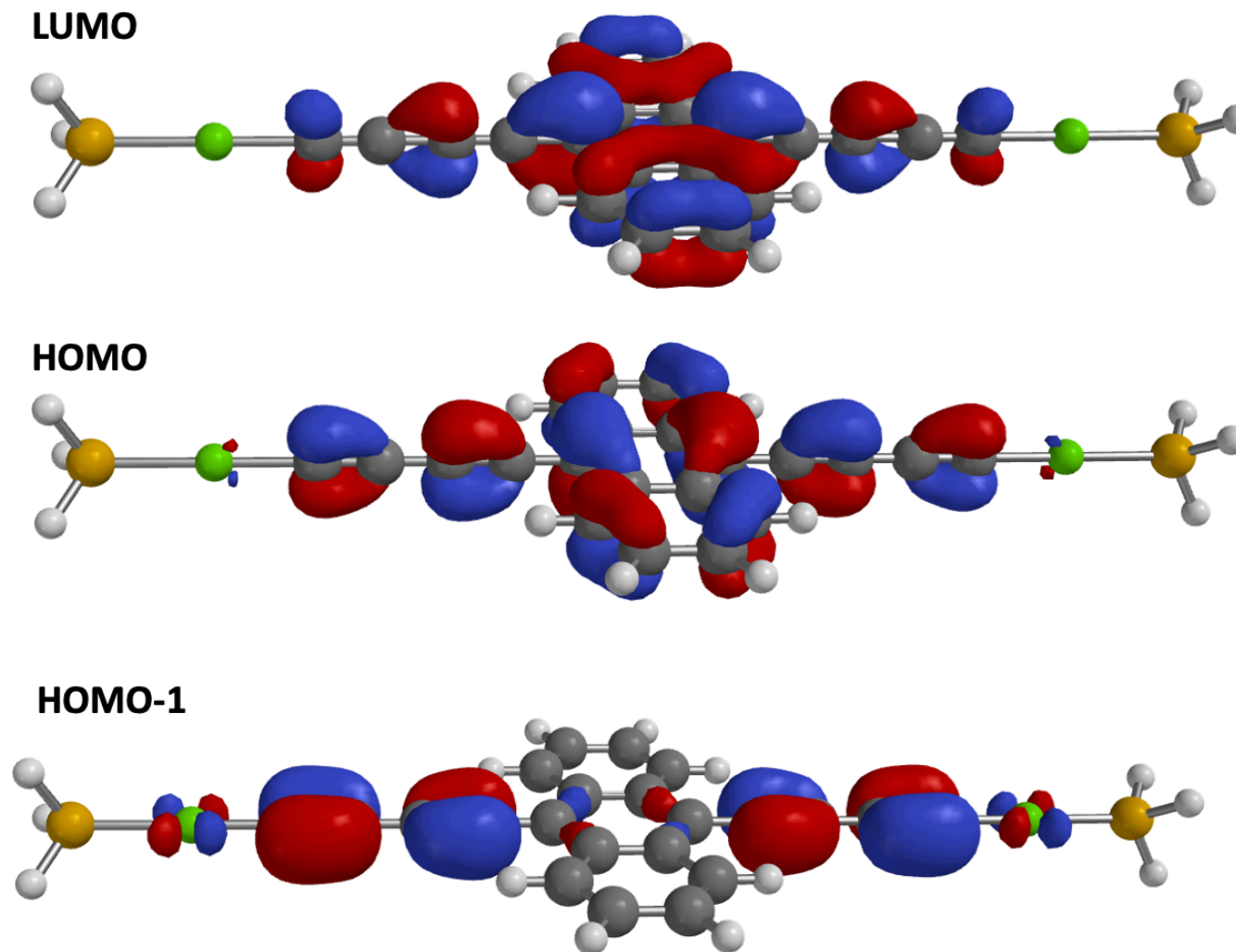


Figure S44. Frontier orbitals of interest for $(\text{H}_3\text{P})\text{Au}-\text{C}\equiv\text{C}-\text{C}\equiv\text{C}-\text{C}_{14}\text{H}_8-\text{C}\equiv\text{C}-\text{C}\equiv\text{C}-\text{Au}(\text{PH}_3)$ ($\omega\text{B97X-D}/6-31\text{G}^*/\text{LANL2D}\zeta(\text{Au})/\text{Gas phase}$)

nm ▾	strength	MO Component	
306.76	0.0000	HOMO-3 → LUMO	40%
		HOMO → LUMO+3	19%
313.45	0.0000	HOMO → LUMO+2	42%
		HOMO-3 → LUMO+1	13%
314.01	0.0000	HOMO → LUMO+1	41%
		HOMO-3 → LUMO+2	12%
		HOMO → LUMO+14	11%
327.63	0.0000	HOMO-2 → LUMO	66%
329.96	0.0000	HOMO-1 → LUMO	70%
436.94	1.1183	HOMO → LUMO	94%

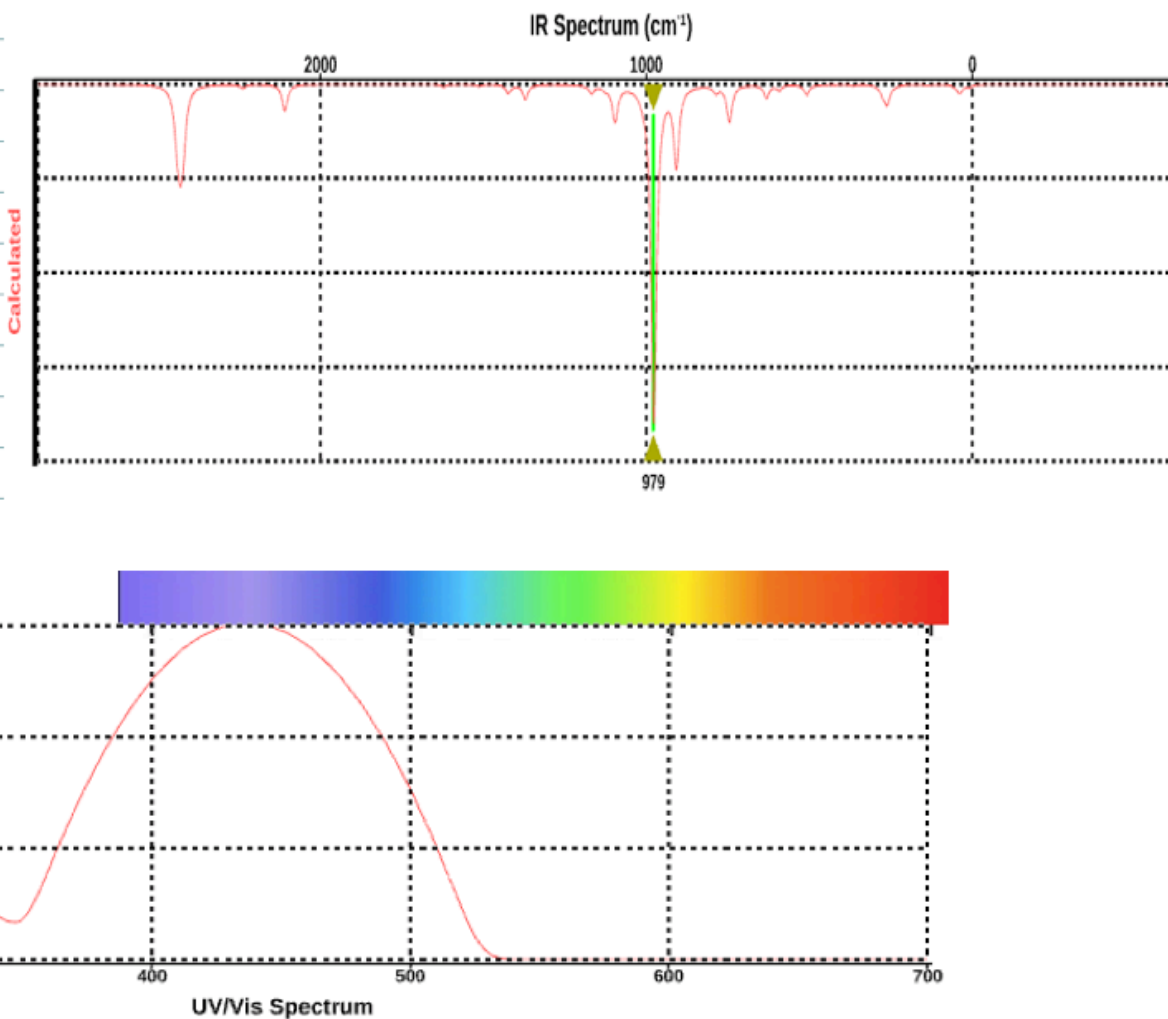


Figure S45. Calculated electronic and infrared spectra of $(\text{H}_3\text{P})\text{Au}-\text{C}=\text{C}-\text{C}=\text{C}-\text{C}_{14}\text{H}_8-\text{C}=\text{C}-\text{C}=\text{C}-\text{Au}(\text{PH}_3)$ ($\omega\text{B97X-D}/6-31\text{G}^*/\text{LANL2D}\zeta(\text{Au})/\text{Gas phase}$). NB: The IR absorption at 979 cm^{-1} that dominates the spectrum corresponds to a δ_{PH} mode.

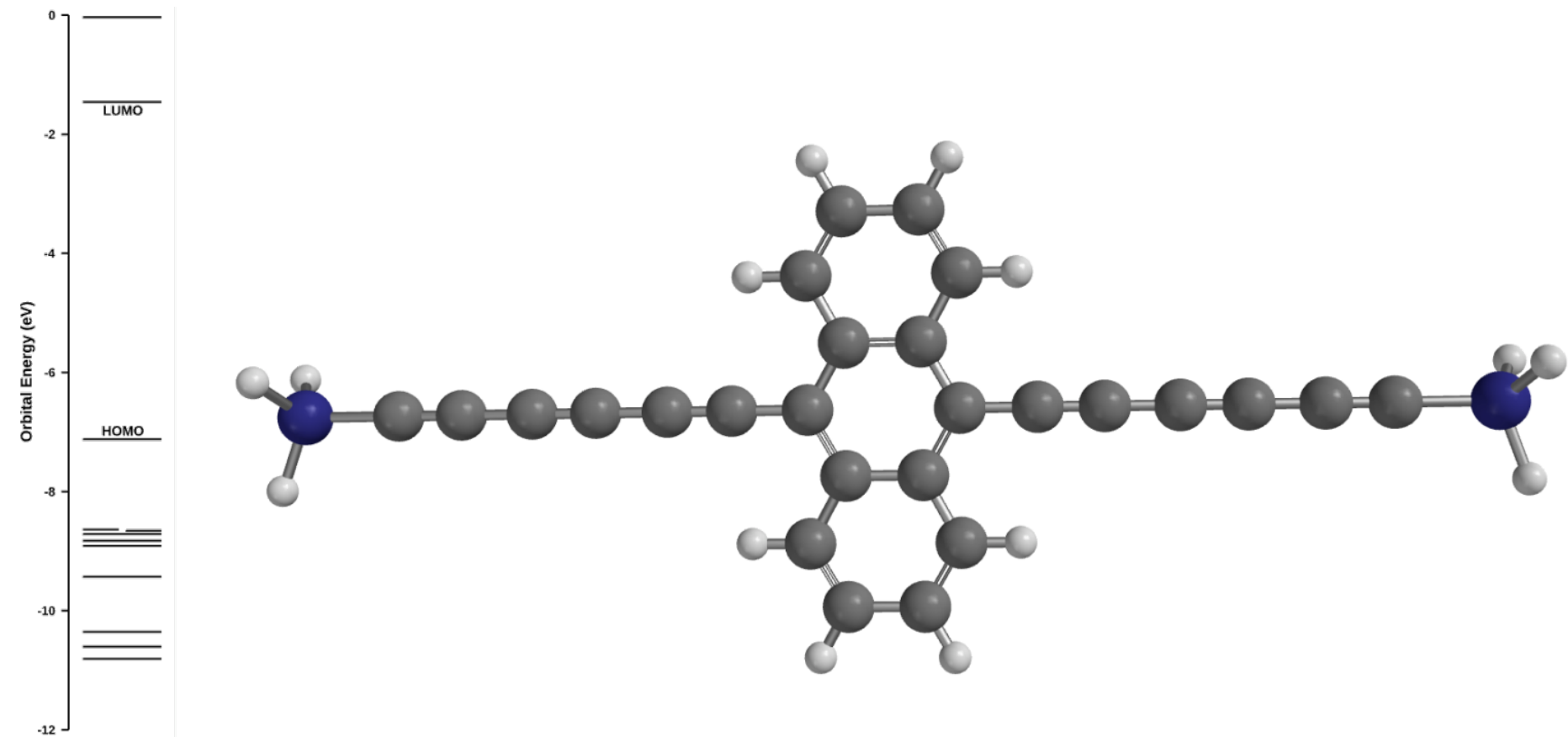


Figure S46. Optimised Geometry and frontier orbitals of $\text{H}_3\text{Si}-\text{C}\equiv\text{C}-\text{C}\equiv\text{C}-\text{C}\equiv\text{C}-\text{C}_{14}\text{H}_8-\text{C}\equiv\text{C}-\text{C}\equiv\text{C}-\text{C}\equiv\text{C}-\text{SiH}_3$ ($\omega\text{B97X-D}/6-31\text{G}^*/\text{Gas phase}$)

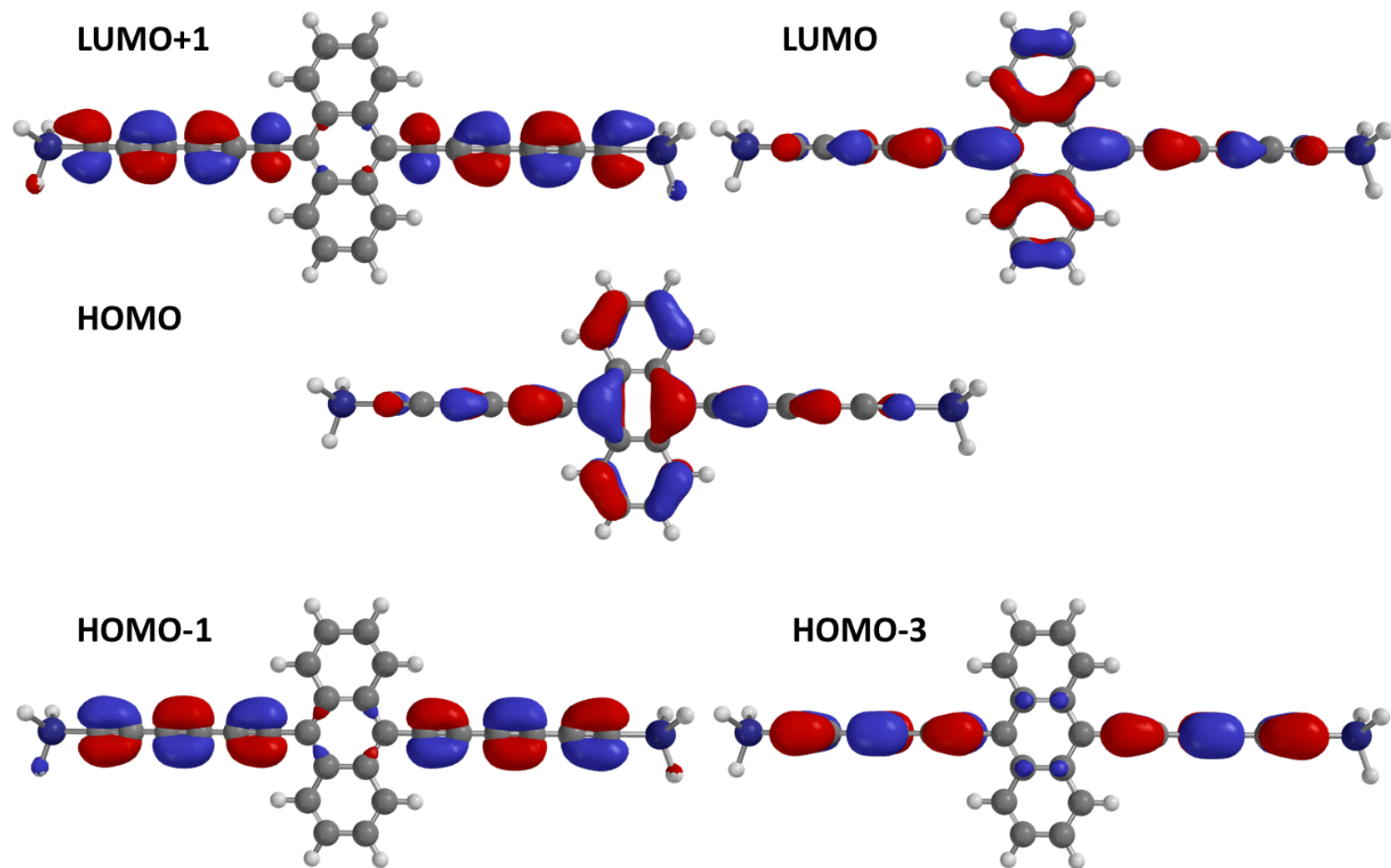


Figure S47. Frontier orbitals of interest for $\text{H}_3\text{Si}-\text{C}\equiv\text{C}-\text{C}\equiv\text{C}-\text{C}\equiv\text{C}-\text{C}_{14}\text{H}_8-\text{C}\equiv\text{C}-\text{C}\equiv\text{C}-\text{C}\equiv\text{C}-\text{SiH}_3$ ($\omega\text{B97X-D}/6-31\text{G}^*/\text{Gas phase}$)

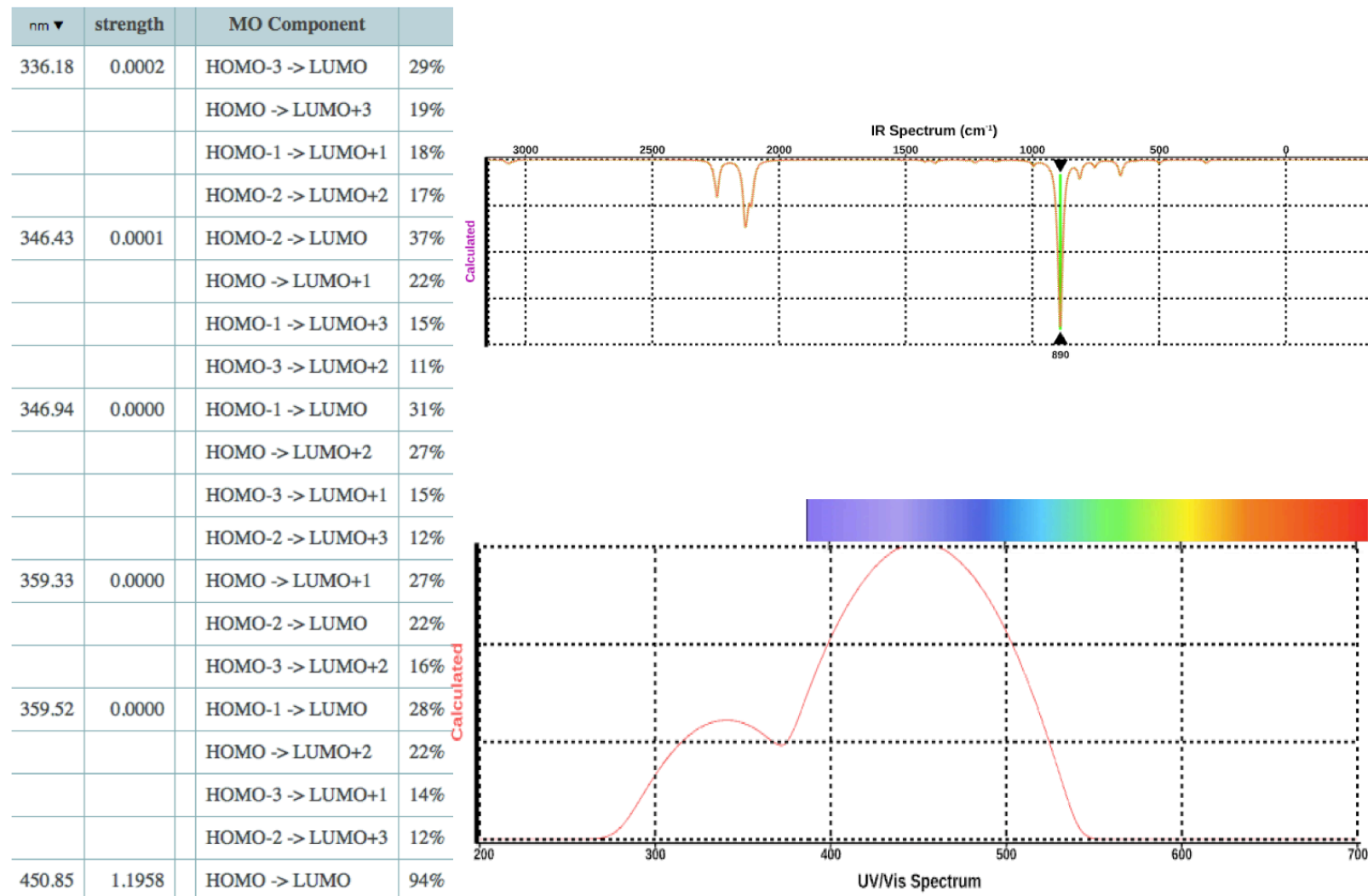


Figure S48. Calculated electronic and infrared spectra of $\text{H}_3\text{Si}-\text{C}\equiv\text{C}-\text{C}\equiv\text{C}-\text{C}\equiv\text{C}-\text{C}_{14}\text{H}_8-\text{C}\equiv\text{C}-\text{C}\equiv\text{C}-\text{C}\equiv\text{SiH}_3$ ($\omega\text{B97X-D}/6-31\text{G}^*/\text{Gas phase}$). NB: The IR absorption at 890 cm^{-1} that dominates the spectrum corresponds to a δ_{SiH} mode

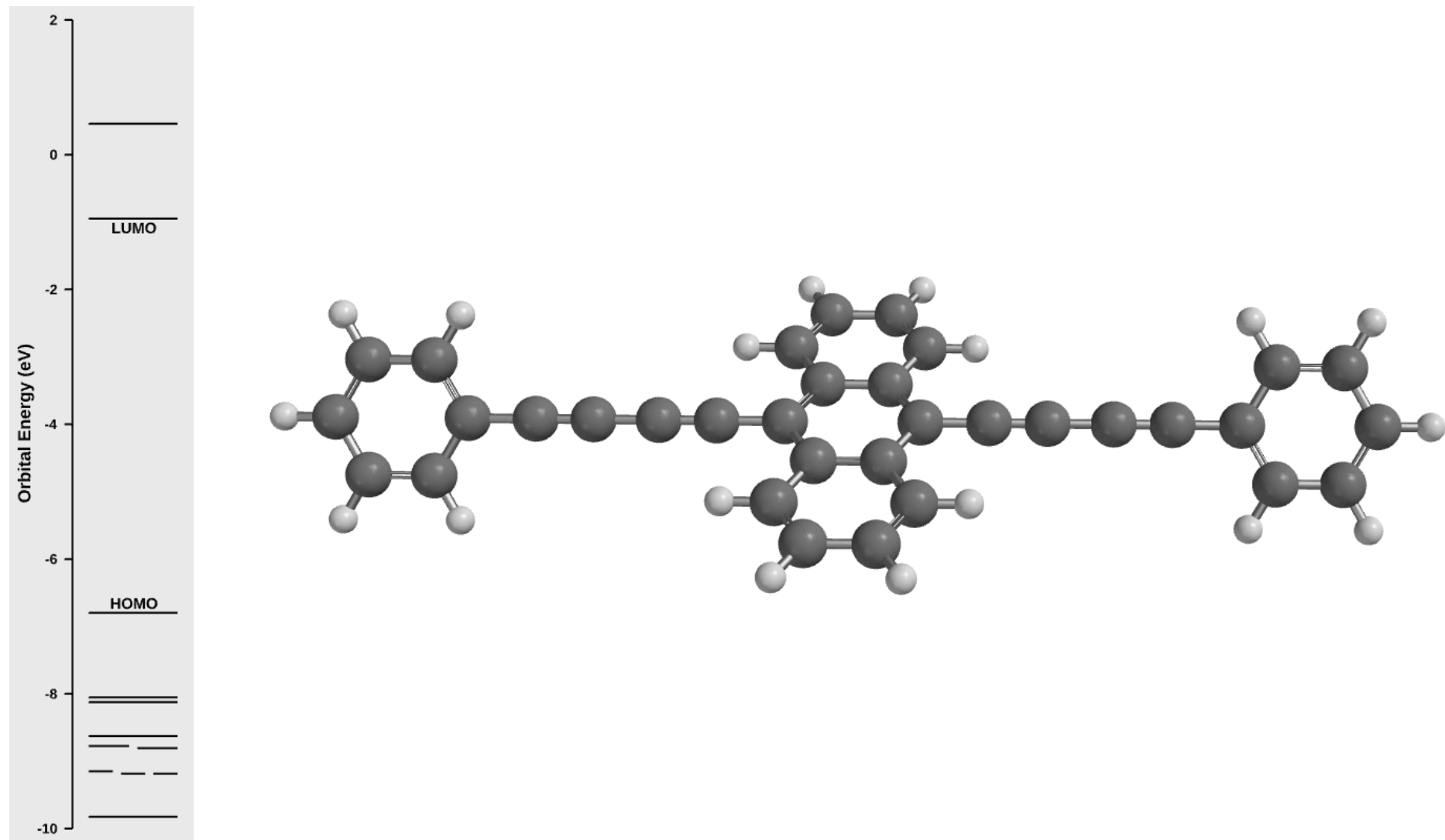


Figure S49. Optimised Geometry and frontier orbitals of $\text{Ph}-\text{C}\equiv\text{C}-\text{C}\equiv\text{C}-\text{C}_{14}\text{H}_8-\text{C}\equiv\text{C}-\text{C}\equiv\text{C}-\text{Ph}$ ($\omega\text{B97X-D}/6-31\text{G}^*/\text{Gas phase}$)

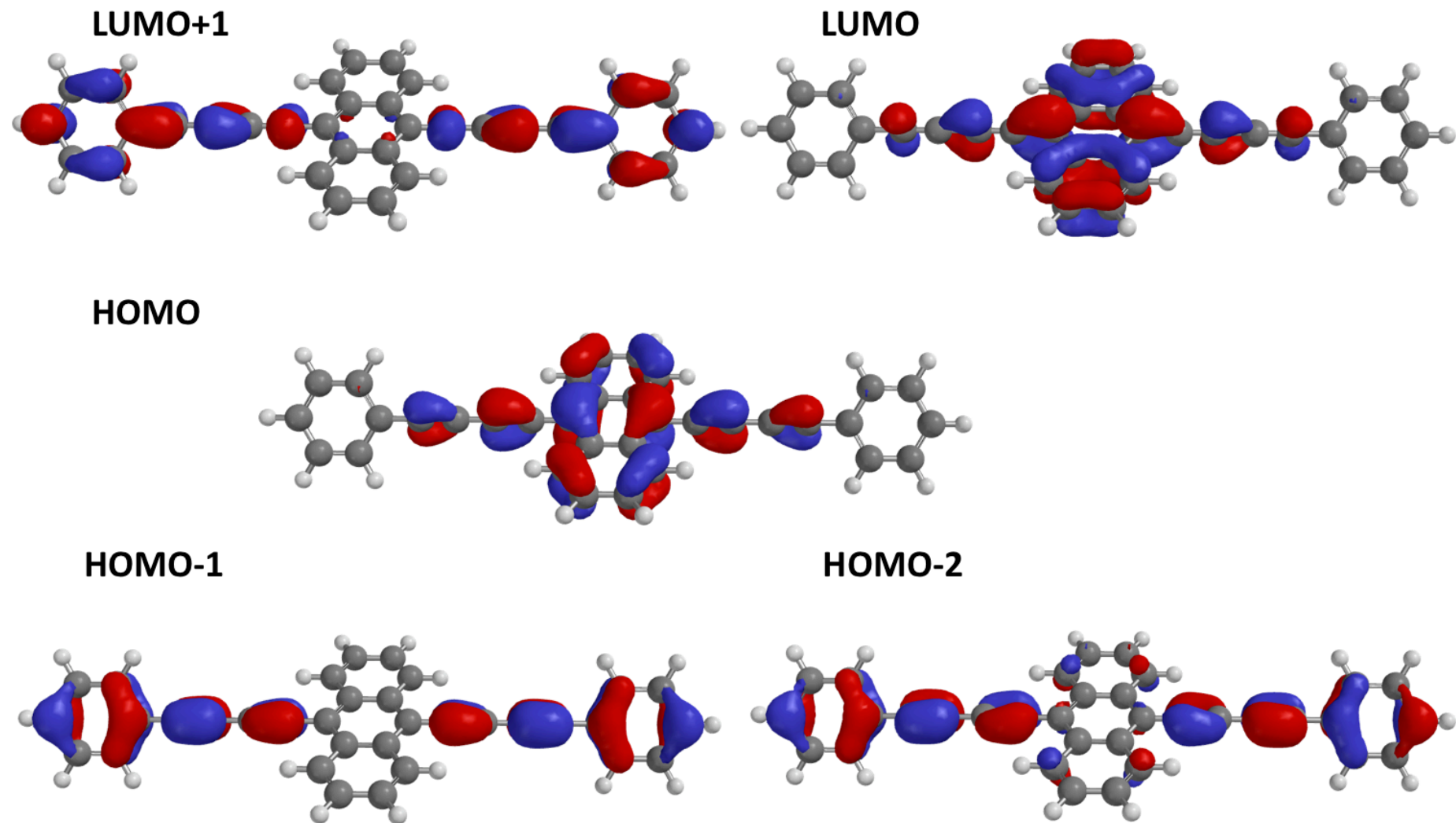
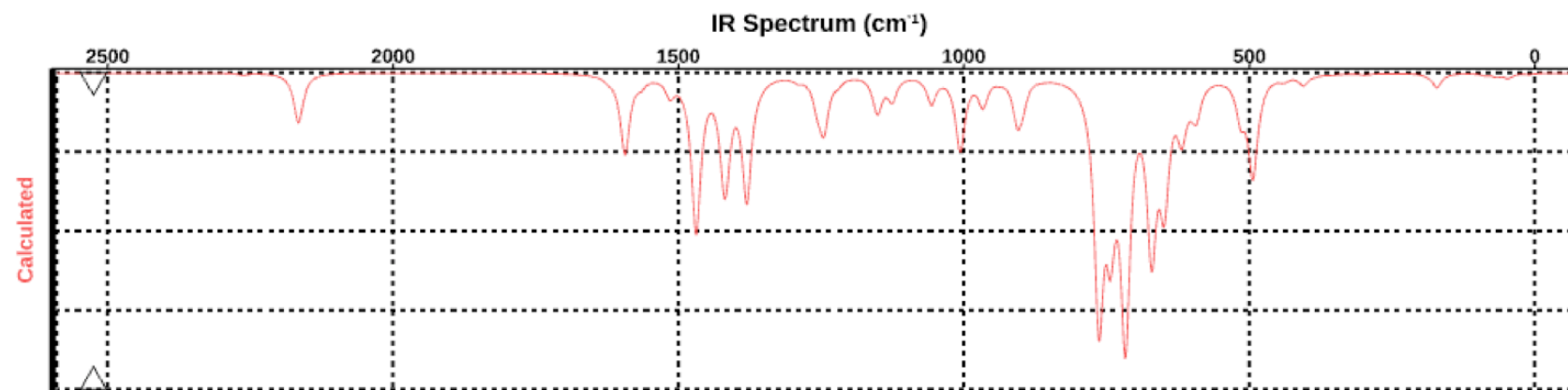


Figure S50. Frontier orbitals of interest for Ph-C#C-C#C-C14H8-C#C-C#C-Ph (ω B97X-D/6-31G*/Gas phase)



nm ▼	strength	MO Component	
304.65	0.1797	HOMO → LUMO+2	51%
		HOMO-5 → LUMO+1	13%
307.19	0.0000	HOMO → LUMO+1	51%
		HOMO-5 → LUMO+2	13%
316.84	0.0215	HOMO-3 → LUMO	59%
		HOMO → LUMO+3	34%
319.63	0.0000	HOMO-1 → LUMO	57%
		HOMO-2 → LUMO	61%
433.54	1.1057	HOMO → LUMO	96%

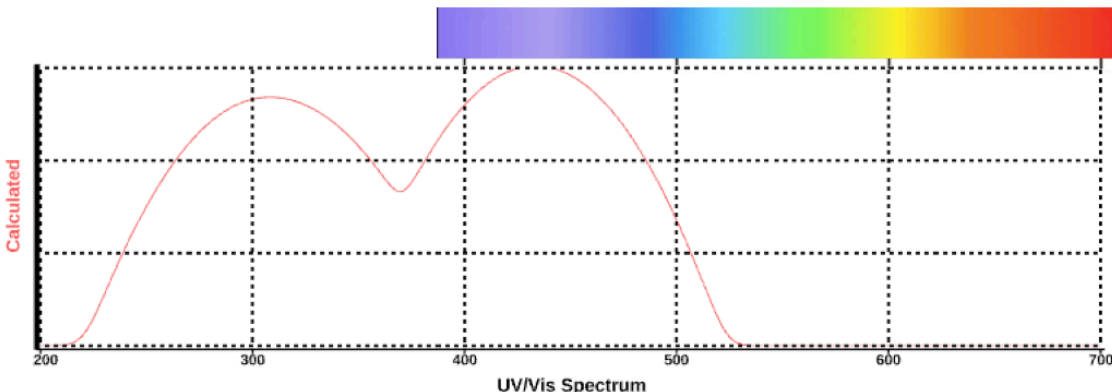


Figure S51. Calculated electronic and infrared spectra of $\text{Ph}-\text{C}\equiv\text{C}-\text{C}\equiv\text{C}-\text{C}_{14}\text{H}_8-\text{C}\equiv\text{C}-\text{C}\equiv\text{C}-\text{Ph}$ ($\omega\text{B97X-D}/6-31\text{G}^*/\text{Gas phase}$)

Cartesian Coordinates and Thermodynamic Data

(a) 9,10-C₁₄H₈(C≡CC≡CPh)₂

Atom	x	y	z
H	4.586897	0.372737	-1.247662
C	3.646452	0.295459	-0.710811
H	2.470335	0.201366	-2.485161
C	2.474085	0.200511	-1.400225
C	2.474059	0.200678	1.400173
C	1.225472	0.098631	-0.714804
C	3.646433	0.295552	0.710735
C	1.225473	0.098706	0.714756
C	0.000334	0.000583	-1.413312
H	4.586869	0.372904	1.247599
H	2.470324	0.201673	2.485113
C	-1.224765	-0.097232	-0.714807
C	-2.473172	-0.199227	-1.400307
C	-1.224767	-0.097137	0.714834
H	-2.469466	-0.199784	2.485248
C	0.000344	0.000769	1.413301
C	-3.645459	-0.294238	-0.710804
H	-2.469442	-0.200209	-2.485224
H	-4.585922	-0.371707	-1.247626
C	-3.645480	-0.294101	0.710851
H	-4.585956	-0.371454	1.247660
C	-2.473201	-0.198994	1.400336
C	0.000417	0.000018	-2.836531
C	0.000520	0.000326	-4.051669
C	-0.000045	-0.000175	-5.420242
C	-0.000138	-0.000225	-6.633940
C	0.000703	0.000715	2.836524
C	0.000566	0.000366	4.051674
C	-0.000041	-0.000015	5.420250
C	-0.000177	0.000062	6.633946
C	-0.000247	-0.000324	8.062334
C	-0.000732	-0.001104	10.855943
C	-0.829801	0.881832	8.770094
C	0.829112	-0.882874	8.769853
C	0.825453	-0.879736	10.158698
C	-0.826656	0.877895	10.158911
H	-1.469706	1.564797	8.220820
H	1.469168	-1.565619	8.220476
H	1.469460	-1.566575	10.699340
H	-1.470870	1.564427	10.699643
H	-0.000918	-0.001373	11.941703
C	-0.000270	-0.000352	-8.062327
C	-0.000647	-0.000957	-10.855930
C	0.829179	-0.882780	-8.769878
C	-0.829907	0.881765	-8.770049
C	-0.826705	0.877909	-10.158874
C	0.825581	-0.879559	-10.158711
H	1.469252	-1.565496	-8.220492
H	-1.469929	1.564631	-8.220784

H	-1.470972	1.564397	-10.699612
H	1.469677	-1.566309	-10.699344
H	-0.000771	-0.001153	-11.941689

Thermodynamic Properties at 298.15 K

Zero Point Energy :	998.36	kJ/mol	(ZPE)
Temperature Correction :	62.04	kJ/mol	(vibration + gas law + rotation + translation)
Enthalpy Correction :	1060.40	kJ/mol	(ZPE + temperature correction)
Enthalpy :	-1305.385870	au	(Electronic Energy + Enthalpy Correction)
Entropy :	635.84	J/mol•K	
Gibbs Energy :	-1305.458075	au	(Enthalpy - T*Entropy)
C _v :	461.46	J/mol•K	

(b) 9,10-C₁₄H₈(C≡CC≡CC≡CSiH₃)₂

Atom	x	y	z
H	4.599005	0.001111	-1.248086
C	3.655592	0.000818	-0.711195
H	2.477285	0.001696	-2.485995
C	2.479600	0.001135	-1.401114
C	2.479780	-0.000251	1.400428
C	1.227899	0.000768	-0.714887
C	3.655676	0.000058	0.710249
C	1.227995	0.000148	0.714449
C	-0.003024	0.000962	-1.411044
H	4.599179	-0.000232	1.247005
H	2.477691	-0.000829	2.485318
C	-1.233839	0.000649	-0.714675
C	-2.485485	0.000854	-1.400762
C	-1.233735	0.000082	0.714739
H	-2.483000	-0.000872	2.485923
C	-0.002846	-0.000091	1.410866
C	-3.661299	0.000466	-0.710555
H	-2.483376	0.001347	-2.485678
H	-4.604823	0.000631	-1.247283
C	-3.661198	-0.000185	0.710983
H	-4.604654	-0.000505	1.247822
C	-2.485287	-0.000362	1.401018
C	-0.002879	0.000698	-2.832276
C	-0.001227	0.000703	-4.048614
C	0.000535	0.000418	-5.411713
C	0.001944	0.000487	-6.628965
C	-0.002416	-0.000824	2.832105
C	-0.001211	-0.000690	4.048490
C	0.000420	-0.000864	5.411587
C	0.002433	-0.001137	6.628845
C	0.004291	-0.000304	-7.994396
C	0.005955	-0.000600	-9.213076
C	0.003532	-0.000311	7.994753

C	0.004809	-0.000283	9.213337
Si	0.005966	-0.000992	-11.040534
H	-0.692486	1.209609	-11.532498
H	-0.693792	-1.211124	-11.532006
H	1.404034	-0.001874	-11.531512
Si	0.005491	0.000003	11.040762
H	-0.693103	-1.210369	11.533238
H	-0.692878	1.210599	11.533000
H	1.403448	-0.000542	11.531946

Thermodynamic Properties at 298.15 K

Zero Point Energy :	716.59	kJ/mol	(ZPE)
Temperature Correction :	61.36	kJ/mol	(vibration + gas law + rotation + translation)
Enthalpy Correction :	777.96	kJ/mol	(ZPE + temperature correction)
Enthalpy :	-1577.145211	au	(Electronic Energy + Enthalpy Correction)
Entropy :	634.39	J/mol•K	
Gibbs Energy :	-1577.217251	au	(Enthalpy - T*Entropy)
C _v :	434.83	J/mol•K	

(c) 9,10-C₁₄H₈(C≡CC≡CAuPH₃)₂

Atom	x	y	z
H	-4.600613	0.001149	-1.248494
C	-3.657143	0.001571	-0.710898
H	-2.474705	0.002042	-2.485149
C	-2.480668	0.002067	-1.400095
C	-2.480659	0.002087	1.400027
C	-1.227652	0.002478	-0.714797
C	-3.657137	0.001584	0.710860
C	-1.227648	0.002483	0.714720
C	-0.000160	0.002870	-1.416934
H	-4.600599	0.001178	1.248467
H	-2.474678	0.002081	2.485080
C	1.227335	0.002481	-0.714803
C	2.480348	0.002082	-1.400107
C	1.227338	0.002480	0.714714
H	2.474376	0.002049	2.485068
C	-0.000153	0.002874	1.416859
C	3.656826	0.001582	-0.710916
H	2.474380	0.002072	-2.485161
H	4.600294	0.001174	-1.248516
C	3.656826	0.001573	0.710843
H	4.600292	0.001153	1.248444
C	2.480352	0.002071	1.400015
C	-0.000164	0.003836	-2.839936
C	-0.000163	0.004919	-4.055763
C	-0.000151	0.005528	-5.425409
C	-0.000145	0.005953	-6.647271
C	-0.000149	0.003841	2.839975
C	-0.000150	0.004929	4.055873

C	-0.000162	0.005525	5.425203
C	-0.000167	0.005956	6.647145
Au	-0.000109	0.003055	-8.631874
Au	-0.000201	0.003053	8.632082
P	-0.000285	-0.007627	10.960148
H	-0.214239	-1.233147	11.610813
H	-0.951202	0.781551	11.626835
H	1.163054	0.411626	11.625259
P	-0.000024	-0.007622	-10.959925
H	1.172943	-0.416203	-11.614343
H	-0.231894	1.205058	-11.628638
H	-0.933347	-0.823411	-11.619405

Thermodynamic Properties at 298.15 K

Zero Point Energy :	684.73	kJ/mol	(ZPE)
Temperature Correction :	60.66	kJ/mol	(vibration + gas law + rotation + translation)
Enthalpy Correction :	745.39	kJ/mol	(ZPE + temperature correction)
Enthalpy :	-1799.591814	au	(Electronic Energy + Enthalpy Correction)
Entropy :	650.51	J/mol•K	
Gibbs Energy :	-1799.665686	au	(Enthalpy - T*Entropy)
C _v :	419.72	J/mol•K	

(d) 9,10-C₁₄H₈(C≡CC≡CAuCO)₂

Atom	x	y	z
H	4.599905	0.002061	-1.245355
C	3.656095	0.001755	-0.708692
H	2.476349	0.001842	-2.483915
C	2.480305	0.001637	-1.398911
C	2.478504	0.001180	1.401745
C	1.227354	0.001369	-0.714032
C	3.655159	0.001424	0.712941
C	1.226429	0.001201	0.715343
C	-0.000786	0.001175	-1.414607
H	4.598276	0.001430	1.250840
H	2.473288	0.000964	2.486726
C	-1.229912	0.001040	-0.715522
C	-2.482127	0.000981	-1.401853
C	-1.230841	0.000879	0.713890
H	-2.479933	0.000342	2.483761
C	-0.002619	0.000916	1.414433
C	-3.658846	0.000809	-0.713052
H	-2.476883	0.001178	-2.486855
H	-4.601976	0.000876	-1.250943
C	-3.659791	0.000498	0.708550
H	-4.603608	0.000283	1.245209
C	-2.483936	0.000547	1.398734
C	0.000404	0.000714	-2.837033
C	0.000510	0.000267	-4.052761
C	0.000490	0.000069	-5.420927

C	-0.001122	0.000386	-6.642365
C	-0.002828	0.000561	2.836847
C	-0.001242	0.001229	4.052567
C	-0.000247	0.002915	5.420732
C	0.001036	0.005385	6.642169
Au	-0.001129	-0.000660	-8.616647
Au	0.003964	0.006191	8.616416
C	0.009575	-0.003127	10.570578
O	0.015160	-0.017442	11.704670
C	0.004040	-0.004163	-10.569338
O	0.010983	-0.007504	-11.703344

Thermodynamic Properties at 298.15 K

Zero Point Energy :	587.49	kJ/mol	(ZPE)
Temperature Correction :	56.96	kJ/mol	(vibration + gas law + rotation + translation)
Enthalpy Correction :	644.45	kJ/mol	(ZPE + temperature correction)
Enthalpy :	-1339.940169	au	(Electronic Energy + Enthalpy Correction)
Entropy :	626.83	J/mol•K	
Gibbs Energy :	-1340.011352	au	(Enthalpy - T*Entropy)
C _v :	391.77	J/mol•K	